Foundation of a Mathematical Model of Physical Reality

By J.A.J. van Leunen

Last modified: 9 november 2015

Abstract

This paper starts from the idea that physical reality implements a network of a small number of mathematical structures. Only in that way can be explained that observations of physical reality fit so well with mathematical methods.

The mathematical structures do not contain mechanisms that ensure coherence. Thus apart from the network of mathematical structures a model of physical reality must contain mechanisms that manage coherence such that dynamical chaos is prevented.

Reducing complexity appears to be the general strategy. The structures appear in chains that start with a foundation. The strategy asks that especially in the lower levels, the subsequent members of the chain emerge with inescapable self-evidence from the previous member. The chains are interrelated and in this way they enforce mutual restrictions.

As a consequence the lowest levels of a corresponding mathematical model of physical reality are rather simple and can easily be comprehended by skilled mathematicians.

In order to explain the claimed setup of physical reality, the paper investigates the foundation of the major chain. That foundation is a skeleton relational structure and it was already discovered and introduced in 1936.

The paper does not touch more than the first development levels. The base model that is reached in this way puts already very strong restrictions to more extensive models.

As part of the investigation the paper compares two sets of differential equations that both give a description of the behavior of physical fields.

Some of the features of the base model are investigated and compared with results of contemporary physics.

If the model introduces new science, then it has fulfilled its purpose.

Contents

1 Introduction

Physical reality is that what physicists try to model in their theories. It appears that observations of features and phenomena of physical reality can often be explained by mathematical structures and mathematical methods. This is not strange, because these mathematical structures and methods are often designed by using examples that are obtained by carefully observing reality as a guidance.

This leads to the unorthodox idea that physical reality itself incorporates a small set of mathematical structures. In that case physical reality will show the features and phenomena of these structures.

In humanly developed mathematics, mathematical structures appear in chains that start from a foundation and subsequent members of the chain emerge with inescapable self-evidence from the previous member. The chains are often interrelated and impose then mutual restrictions. It is obvious to expect a similar setup for the structures that are maintained by physical reality.

Physical reality is known to show coherence. Its behavior is far from chaotic. The incorporated mathematical structures do not contain mechanisms that ensure coherence. The structures may only help to ensure coherence. Thus apart from the network of mathematical structures a model of physical reality must contain mechanisms that manage coherence such that dynamical chaos is prevented.

In physical reality, reducing complexity appears to be the general strategy.

One chain is expected to play a major role and its foundation can be viewed as the major foundation of the investigated model of physical reality. The discovery of this foundation is essential for explaining how the network of incorporated mathematical structures is configured.

2 Physical theories

Physical theories support their application by describing the applied structures and the applied phenomena. The aim of these theories is not the explanation of the origins of these structures and phenomena. The fact that the described structures and phenomena can be applied means that these subjects can be observed. This is the main reason behind the claim of what is called the scientific method. ***The scientific method*** requires that every significant physical statement must be verified by experiments.

This paper investigates deeper than physical theories tend to do. It explores the potential relation between mathematical theories and physical reality in order to explain structures and phenomena that follow from a selected set of mathematical foundations.

It will not be possible to prove that the corollaries of the mathematical models will represent the observable structures and phenomena of the physical model. On the other hand, the mathematical model might enhance the insight into corresponding physical models.

For example this paper applies quaternionic differential calculus as alternative for or addition to Maxwell based differential calculus and it applies quaternionic Hilbert spaces in ways that are not exploited by current physical theories.

3 The major chain

3.1 The foundation

This paper uses the skeleton relational structure that in 1936 was discovered by Garret Birkhoff and John von Neumann as the major foundation of the model. Birkhoff and von Neumann named it "quantum logic"[1].

The ~25 axioms that define an orthocomplemented weakly modular lattice form the first principles on which according to this paper the model of physical reality is supposed to be built [2]. Another name for this lattice is ***orthomodular lattice***. Quantum logic has this lattice structure. Classical logic has a slightly different lattice structure. Classical logic has the structure of an orthocomplemented modular lattice. Due to this resemblance, the discoverers of the orthomodular lattice gave quantum logic its name. The treacherous name "quantum logic" has invited many scientists to deliberate in vain about the significance of the elements of the orthomodular lattice as logical propositions. For our purpose it is better to interpret the elements of the orthomodular lattice as ***construction elements*** rather than as ***logic propositions***.

By taking this point of view, the selected foundation can be considered as part of a recipe for modular construction. What is missing are the binding mechanism and a way to hide part of the relations that exist inside the modules from the outside of the modules. That functionality is supposed to be realized in higher levels of the model.

Thus, being a member of an orthomodular lattice is not enough in order to become a member of a modular system.

3.2 Extending the major chain

The next level of the major chain of mathematical structures ***emerges with inescapable self-evidence*** from the selected foundation.

Not only quantum logic forms an orthomodular lattice, but also the set of closed subspaces of an infinite dimensional separable Hilbert space forms an orthomodular lattice [1].

Where the orthomodular lattice was discovered in the thirties, the Hilbert space was introduced shortly before that time [3]. The Hilbert space is a vector space that features an inner product. The orthomodular lattice that is formed by its set of subspaces makes the Hilbert space a very special vector space.

The Hilbert space adds extra functionality to the orthomodular lattice. This extra functionality concerns the superposition principle and the possibility to store numeric data in eigenspaces of normal operators. In the form of Hilbert vectors the Hilbert space features a finer structure than the orthomodular lattice has.

These features caused that Hilbert spaces were quickly introduced in the development of quantum physics.

Numbers do not exist in the realm of a pure orthomodular lattice. Via the Hilbert space, number systems emerge into the model. Number systems do not find their foundation in the major chain. Instead they belong to another chain of mathematical structures. The foundation of that chain concerns mathematical sets.

The Hilbert space can only handle members of a division ring for specifying superposition coefficients, for the eigenvalues of its operators and for the values of its inner products. Only three

suitable division rings exist: the real numbers, the complex numbers and the quaternions. These facts were already known in the thirties but became a thorough mathematical prove in the second half of the twentieth century [4].

Separable Hilbert spaces act as structured storage media for discrete data that can be stored in real numbers, complex numbers or quaternions. Quaternions enable the storage of 1+3D dynamic geometric data that have an Euclidean geometric structure.

The qualification “separable” requests that eigenspaces of operators are countable. This means that eigenvalues are restricted to the rational versions of the supported number systems.

The confinement to division rings puts strong restrictions onto the model. These restrictions reduce the complexity of the whole model.

Thus, selecting a skeleton relational structure that is an orthomodular lattice as the foundation of the model already puts significant restrictions to the model. On the other hand, as can be shown, this choice promotes modular construction. In this way it eases system configuration and the choice significantly reduces the relational complexity of the final model. Quaternions and their notations are treated in the appendix.

4 Consequences of the currently obtained model

The orthomodular lattice can be interpreted as a ***part of a recipe for modular construction***. What is missing are means to ***bind modules*** and means to ***hide relations*** that stay inside the module from the outside of the module. This functionality must be supplied by extensions of the model. It is partly supplied by the superposition principle, which is introduced via the separable Hilbert space.

The current model does not yet support coherent dynamics and it does not support continuums. The selected foundation and its extension to a separable Hilbert space can be interpreted in the following ways:

- Each discrete construct in this model is supposed to expose the skeleton relational structure that is defined as an orthomodular lattice.
- Each discrete construct in this model is either a module or a modular system.
- Every discrete construct in this model can be represented by a closed subspace of a single infinite dimensional separable quaternionic Hilbert space.
- Every module and every modular system in this model can be represented by a closed subspace of a single infinite dimensional separable quaternionic Hilbert space.

However

- Not every closed subspace of the separable Hilbert space represents a module or a modular system.

Modular construction eases system design and system configuration. Modular construction handles its resources in a very economically way. With sufficient resources present it can generate very complicated constructs.

The modular construction recipe is certainly the most influential rule that exists in the generation of physical reality. Even without intelligent design it achieved the construction of intelligent species.

5 Supporting continuums

The separable Hilbert space can only handle discrete numeric data. Physical reality also supports continuums. The eigenspaces of the operators of the separable Hilbert space are countable. Continuums are not countable. Thus, separable Hilbert spaces cannot support continuums.

Soon after the introduction of the Hilbert space, scientists tried to extend the separable Hilbert space to a non-separable version that supports operators, which feature continuums as eigenspaces. With his bra-ket notation for Hilbert vectors and operators and by introducing generic functions, such as the Dirac delta function, Paul Dirac introduced ways to handle continuums [5]. This approach became proper mathematical support in the sixties when the Gelfand triple was introduced [6].

Every infinite dimensional separable Hilbert space owns a Gelfand triple. In fact the separable Hilbert space can be seen as ***embedded*** inside this Gelfand triple. How this embedding occurs in mathematical terms is still obscure. It appears that the embedding process allows a certain amount of freedom that is exploited by the mechanisms, which are contained in physical reality and that have the task to ensure spatial and dynamic coherence. These mechanisms apply ***stochastic operators*** in order to perform their functionality.

This paper introduces methods that relate a category of operators, which reside in the separable Hilbert space and corresponding operators, which reside in the Gelfand triple to continuous functions and their parameter spaces. These methods are based on Dirac's bra-ket notation. These methods relate the separable Hilbert space and its Gelfand triple in a more strict way than embedding pursues.

In the separable Hilbert space the closed subspaces have a well-defined numeric dimension. In contrast, in the non-separable companion the dimension of closed subspaces is in general not defined. The embedding of subspaces of the separable Hilbert space in a subspace of the non-separable Hilbert space that represents an encapsulating composite will at least partly hide the characteristics and interrelations of embedded constituents. This hiding is required for constituents of modular systems.

Subspaces that represent continuum eigenspaces cannot have a countable dimension. They certainly cannot have a finite dimension. In fact the dimension of such subspaces makes little sense.

In this paper we usually ignore the fact that operators that have countable eigenspaces also have an equivalent in the Gelfand triple. One may ask why reality needs the separable Hilbert spaces when the Gelfand triple can handle both discrete and continuum data. The reason is that all or most of the mechanisms that control reality do not act on the Gelfand triple. These mechanisms only control the separable Hilbert space. These mechanisms work in a stepwise fashion that is supported by stochastic operators, which only reside in the separable Hilbert space. Stochastic processes supply the eigenvalues of these operators. The non-separable Hilbert spaces appear to take care of the support of the continuums.

1 Quaternionic Hilbert spaces

Separable Hilbert spaces are linear vector spaces in which an inner product is defined. This inner product relates each pair of Hilbert vectors. The value of that inner product must be a member of a division ring. Suitable division rings are real numbers, complex numbers and quaternions. This paper uses quaternionic Hilbert spaces [2][3][4].

Paul Dirac introduced the bra-ket notation that eases the formulation of Hilbert space habits [5].

$$\langle x|y\rangle = \langle y|x\rangle^* \quad (1)$$

$$\langle x+y|z\rangle = \langle x|z\rangle + \langle y|z\rangle \quad (2)$$

$$\langle \alpha x|y\rangle = \alpha\, \langle x|y\rangle \quad (3)$$

$$\langle x|\alpha y\rangle = \langle x|y\rangle\, \alpha^* \quad (4)$$

$\langle x|$ is a bra vector. $|y\rangle$ is a ket vector. α is a quaternion.

This paper considers Hilbert spaces as no more and no less than structured storage media for dynamic geometrical data that have an Euclidean signature. Quaternions are ideally suited for the storage of such data. Quaternionic Hilbert spaces are described in “Quaternions and quaternionic Hilbert spaces” [6].

The operators of separable Hilbert spaces have countable eigenspaces. Each infinite dimensional separable Hilbert space owns a Gelfand triple. The Gelfand triple embeds this separable Hilbert space and offers as an extra service operators that feature continuums as eigenspaces. In the corresponding subspaces the definition of dimension loses its sense.

1.1 Tensor products

The tensor product of two quaternionic Hilbert spaces is a real Hilbert space [7]. For that reason this model does not apply tensor products. As a consequence Fock spaces are not applied in this paper.

Instead the paper represents the whole model by a single infinite dimensional separable quaternionic Hilbert space and its companion Gelfand triple. Elementary objects and their composites will be represented by subspaces of the separable Hilbert space. Their local living spaces coexist as eigenspaces of dedicated operators.

1.2 Representing continuums and continuous functions

Operators map Hilbert vectors onto other Hilbert vectors. Via the inner product the operator T may be linked to an adjoint operator $T^\dagger$.

$$\langle Tx|y\rangle \equiv \langle x|T^\dagger y\rangle \quad (1)$$

$$\langle Tx|y\rangle = \langle y|Tx\rangle^* = \langle T^\dagger y|x\rangle^* \quad (2)$$

A linear quaternionic operator T, which owns an adjoint operator $T^\dagger$ is normal when

$$T^\dagger T \;=\; T\,T^\dagger \quad (3)$$

$T_0 = (T + T^\dagger)/2$ is a self adjoint operator and $\boldsymbol{T} = (T - T^\dagger)/2$ is an imaginary normal operator. Self adjoint operators are also Hermitian operators. Imaginary normal operators are also anti-Hermitian operators.

By using what we will call ***reverse bra-ket notation***, operators that reside in the Hilbert space and correspond to continuous functions, can easily be defined by starting from an orthonormal base of vectors. In this base the vectors are normalized and are mutually orthogonal. The vectors span a subspace of the Hilbert space. We will attach eigenvalues to these base vectors via the reverse bra-ket notation. This works both in separable Hilbert spaces as well as in non-separable Hilbert spaces.

Let $\{q_i\}$ be the set of rational quaternions in a selected quaternionic number system and let $\{|q_i\rangle\}$ be the set of corresponding base vectors. They are eigenvectors of a normal operator $\mathcal{R} = |q_i\rangle q_i \langle q_i|$. Here we enumerate the base vectors with index ⍰.

$$\mathcal{R} = |q_i\rangle q_i \langle q_i| \tag{4}$$

$\mathcal{R}$ is the configuration parameter space operator.

$\mathcal{R}_0 = (\mathcal{R} + \mathcal{R}^\dagger)/2$ is a self-adjoint operator. Its eigenvalues can be used to arrange the order of the eigenvectors by enumerating them with the eigenvalues. The ordered eigenvalues can be interpreted as ***progression values***.

$\boldsymbol{\mathcal{R}} = (\mathcal{R} - \mathcal{R}^\dagger)/2$ is an imaginary operator. Its eigenvalues can also be used to order the eigenvectors. The eigenvalues can be interpreted as ***spatial values*** and can be ordered in several ways.

Let $f(q)$ be a mostly continuous quaternionic function. Now the reverse bra-ket notation defines operator f as:

$$f = |q_i\rangle f(q_i) \langle q_i| \tag{5}$$

f defines a new operator that is based on function $f(q)$. Here we suppose that the target values of f belong to the same version of the quaternionic number system as its parameter space does.

Operator f has a countable set of discrete quaternionic eigenvalues.

For this operator the reverse bra-ket notation is a shorthand for

$$\langle x|f\ y\rangle = \sum_i \langle x|q_i\rangle f(q_i) \langle q_i|y\rangle \tag{6}$$

In a non-separable Hilbert space, such as the Gelfand triple, the continuous function $\mathcal{F}(q)$ can be used to define an operator, which features a continuum eigenspace.

$$\mathcal{F} = |q\rangle \mathcal{F}(q) \langle q| \tag{7}$$

Via the continuous quaternionic function $\mathcal{F}(q)$, the operator $\mathcal{F}$ defines a curved continuum $\mathcal{F}$. This operator and the continuum reside in the Gelfand triple, which is a non-separable Hilbert space.

$$\mathfrak{R} = |q\rangle q \langle q| \tag{8}$$

The function $\mathcal{F}(q)$ uses the eigenspace of the reference operator $\mathfrak{R}$ as a flat parameter space that is spanned by a quaternionic number system $\{q\}$. The continuum $\mathcal{F}$ represents the target space of function $\mathcal{F}(q)$.

Here we no longer enumerate the base vectors with index i. We just use the name of the parameter. If no conflict arises, then we will use the same symbol for the defining function, the defined operator and the continuum that is represented by the eigenspace.

For the shorthand of the reverse bra-ket notation of operator $\mathcal{F}$ the integral over q replaces the summation over q_i.

$$\langle x|\mathcal{F}\ y\rangle = \int_q \langle x|q\rangle \mathcal{F}(q) \langle q|y\rangle\ dq \tag{9}$$

Remember that quaternionic number systems exist in several versions, thus also the operators f and $\mathcal{F}$ exist in these versions. The same holds for the parameter space operators. When relevant, we will use superscripts in order to differentiate between these versions.

Thus, operator $f^x = |q_i^x\rangle f^x(q_i^x)\langle q_i^x|$ is a specific version of operator f. Function $f^x(q_i^x)$ uses parameter space $\mathcal{R}^x$.

Similarly, $\mathcal{F}^x = |q^x\rangle \mathcal{F}^x(q^x)\langle q^x|$ is a specific version of operator $\mathcal{F}$. Function $\mathcal{F}^x(q^x)$ and continuum $\mathcal{F}^x$ use parameter space $\mathfrak{R}^x$. If the operator $\mathcal{F}^x$ that resides in the Gelfand triple $\mathcal{H}$ uses the same defining function as the operator $\mathcal{F}^x$ that resides in the separable Hilbert space, then both operators belong to the same quaternionic ordering version.

In general the dimension of a subspace loses its significance in the non-separable Hilbert space.

The continuums that appear as eigenspaces in the non-separable Hilbert space $\mathcal{H}$ can be considered as quaternionic functions that also have a representation in the corresponding infinite dimensional separable Hilbert space $\mathfrak{H}$. Both representations use a flat parameter space $\mathfrak{R}^x$ or $\mathcal{R}^x$ that is spanned by quaternions. $\mathcal{R}^x$ is spanned by rational quaternions.

The parameter space operators will be treated as reference operators. The rational quaternionic eigenvalues $\{q_i^x\}$ that occur as eigenvalues of the reference operator $\mathcal{R}^x$ in the separable Hilbert space map onto the rational quaternionic eigenvalues $\{q_i^x\}$ that occur as subset of the quaternionic eigenvalues $\{q^x\}$ of the reference operator $\mathfrak{R}^x$ in the Gelfand triple. In this way the reference operator $\mathcal{R}^x$ in the infinite dimensional separable Hilbert space $\mathfrak{H}$ relates directly to the reference operator $\mathfrak{R}^x$, which resides in the Gelfand triple $\mathcal{H}$.

All operators that reside in the Gelfand triple and are defined via a mostly continuous quaternionic function have a representation in the separable Hilbert space.

1.3 Stochastic operators

Stochastic operators do not get their data from a continuous quaternionic function. Instead a stochastic process delivers the eigenvalues. Again these eigenvalues are quaternions and the real parts of these quaternions can be interpreted as progression values. The generated eigenvalues are picked from a selected parameter space.

Stochastic operators only act in a step-wise fashion. Their eigenspace is countable. Stochastic operators may act in a cyclic fashion.

The mechanisms that control the stochastic operator can synchronize the progression values with the model wide progression that is set by a selected reference operator.

Characteristic for stochastic operators is that the imaginary parts of the eigenvalues are not smooth functions of the real values of those eigenvalues.

1.3.1 Density operators

The eigenspace of a stochastic operator may be characterized by a continuous spatial density distribution. In that case the corresponding stochastic process must ensure that this continuous density distribution fits. The density distribution can be constructed afterwards or after each regeneration cycle. Constructing the density distribution involves a reordering of the imaginary parts of the produced eigenvalues. This act will usually randomize the real parts of those eigenvalues. A different operator can then use the continuous density distribution in order to generate its functionality. The old real parts of the eigenvalues may then reflect the reordering. The construction of the density distribution is a pure administrative action that is performed as an aftermath. The constructed density operator represents a continuous function and may reside both in the separable Hilbert space and in the Gelfand triple. The construction of the density function involves a selected parameter space. That parameter space need not be the same as the parameter space from which the stochastic process picked its eigenvalues.

1.4 Fourier spaces

Via the Fourier transform of functions, operators can be defined that represent these Fourier transforms. This also involves a change of the parameter spaces. We will use an accent in order to indicate the Fourier space version of functions.

$$\tilde{f}(\tilde{q}) \Leftrightarrow f(q) \tag{1}$$

The function $\tilde{q}(q)$turns reference operator $\mathcal{R}$ into reference operator $\tilde{\mathcal{R}}$ and reference operator $\mathfrak{R}$ into reference operator $\tilde{\mathfrak{R}}$.

$$\tilde{\mathcal{R}} = |q_i\rangle\tilde{q}(q_i)\langle q_i| \tag{2}$$

$$\tilde{\mathfrak{R}} = |q\rangle\tilde{q}(q)\langle q| \tag{3}$$

These operators define the parameter spaces in Fourier space. In the Gelfand triple, the Fourier transform version $\tilde{f}$ of operator f is defined by:

$$\tilde{f} = |\tilde{q}\rangle\tilde{f}(\tilde{q})\langle\tilde{q}| \tag{4}$$

Similarly in separable Hilbert space:

$$\tilde{f} = |\tilde{q}_i\rangle\tilde{f}(\tilde{q}_i))\langle\tilde{q}_i| \tag{5}$$

1.5 Notations

The reverse bra-ket notation enables the definition of some special operators that play an unique role in the model. We will reserve special symbols for these operators and we will also use special symbols in order to distinguish separable from non-separable Hilbert spaces.

Symbol	Meaning	Applied in	As
$\mathfrak{H}$	Separable Hilbert space	Model	Structured storage
$\mathcal{H}$	Non-separable Hilbert space, Gelfand triple	Model	Structured storage
$\mathcal{R}$	Reference operator	$\mathfrak{H}$	Parameter space
$\mathfrak{R}$	Reference operator	$\mathcal{H}$	Parameter space
$\mathfrak{C}$	Embedding continuum operator	$\mathcal{H}$	Field, function
$\mathfrak{A}$	Symmetry related field operator	$\mathcal{H}$	Field, function
$\mathfrak{S}$	Symmetry center operator	$\mathfrak{H}$	Floating parameter space
$\mathscr{o}$	Coherent swarm operator	$\mathfrak{H}$	Dynamic location distribution
$\mathscr{b}$	Mapped coherent swarm operator	$\mathfrak{H}$	Dynamic location distribution
ρ	Density operator	$\mathcal{H}$	Density function

The defining function in the reverse bra-ket notation enables the definition of operators in both the separable Hilbert space $\mathfrak{H}$and in the Gelfand triple $\mathcal{H}$Still different symbols are used for reference operators $\mathfrak{R}$and $\mathcal{R}$

$\mathscr{o}$is a stochastic operator. $\mathscr{b}$ maps the eigenspace of $\mathscr{o}$in parameter space $\mathcal{R}$ ρ is the corresponding density operator.

2 Change of base

In quaternionic Hilbert space a change of base can be achieved by:

$$\langle x|\tilde{\mathcal{F}}\,y\rangle = \int_{\tilde{q}} \langle x\,|\tilde{q}\rangle \left\{ \int_{q} \langle \tilde{q}|q\rangle \mathcal{F}(q)\langle q|\tilde{q}\rangle\, dq \right\} \langle \tilde{q}|y\rangle\, d\tilde{q} \tag{1}$$

$$= \int_{\tilde{q}} \langle x|\tilde{q}\rangle \tilde{\mathcal{F}}(\tilde{q})\langle \tilde{q}|y\rangle\; d\tilde{q}$$

$$\tilde{\mathcal{F}}(\tilde{q}) = \int_{q} \langle \tilde{q}|q\rangle \mathcal{F}(q)\langle q|\tilde{q}\rangle\; dq \tag{2}$$

$$\tilde{\mathfrak{R}}(\tilde{q}) = \int_{q} \langle \tilde{q}|q\rangle q\langle q|\tilde{q}\rangle\; dq \tag{3}$$

$$\langle x|\tilde{\mathfrak{R}}\,y\rangle = \int_{\tilde{q}} \langle x|\tilde{q}\rangle \tilde{\mathfrak{R}}(\tilde{q})\langle \tilde{q}|y\rangle\; d\tilde{q} \tag{4}$$

$$\tilde{\mathfrak{R}} = |\tilde{q}\rangle\tilde{q}\langle\tilde{q}| \tag{5}$$

However, as we see in the formulas this method merely achieves a rotation of parameter spaces and functions. In the complex number based Hilbert space it would achieve no change at all.

2.1 Fourier transform

A Fourier transform uses a different approach. It is not a direct transform between parameter spaces, but instead it is a transform between sets of mutually orthogonal functions, which are

formed by inner products, which are related to different parameter spaces. The quaternionic Fourier transform exists in three versions. The first two versions have a reverse Fourier transform.

The left oriented Fourier transform is defined by:

$$\tilde{\mathcal{F}}_L(\tilde{q}_L) = \int_q \langle \tilde{q}_L | q \rangle \, \mathcal{F}(q) \; dq \tag{1}$$

Like the functions $\langle q|q'\rangle$ and $\langle \tilde{q}_L|\tilde{q}'_L\rangle$, the functions $\langle \tilde{q}_L|q\rangle$ and $\langle q|\tilde{q}_L\rangle$ form sets of mutually orthogonal functions, as will be clear from:

$$\langle q|q'\rangle = \delta(q-q') \tag{2}$$

$$\langle \tilde{q}_L|\tilde{q}'_L\rangle = \delta(\tilde{q}_L-\tilde{q}'_L) \tag{3}$$

$$\int_{\tilde{q}_L} \langle q'|\tilde{q}_L\rangle\langle \tilde{q}_L|q\rangle \; d\tilde{q}_L = \delta(q-q') \tag{4}$$

$$\int_q \langle \tilde{q}'_L|q\rangle\langle q|\tilde{q}_L\rangle \; dq = \delta(\tilde{q}_L-\tilde{q}'_L) \tag{5}$$

The reverse transform is:

$$\mathcal{F}(q) = \int_{\tilde{q}_L} \langle q|\tilde{q}_L\rangle \tilde{\mathcal{F}}_L(\tilde{q}_L)\, d\tilde{q}_L = \int_{\tilde{q}_L}\int_{q'} \langle q|\tilde{q}_L\rangle\langle \tilde{q}_L|q'\rangle \mathcal{F}(q')\, d\tilde{q}_L\, dq' \tag{6}$$

$$= \int_{q'} \left\{ \int_{\tilde{q}_L} \langle q|\tilde{q}_L\rangle\langle \tilde{q}_L|q'\rangle \, d\tilde{q}_L \right\} \mathcal{F}(q')\, dq' = \int_{q'} \delta(q-q')\mathcal{F}(q')\, dq'$$

The reverse bra-ket form of the operator $\tilde{\mathcal{F}}_L$ equals:

$$\tilde{\mathcal{F}}_L = |\tilde{q}_L\rangle \tilde{\mathcal{F}}_L(\tilde{q}_L)\langle \tilde{q}_L| \tag{7}$$

Operator $\widetilde{\mathfrak{R}}_L$ provides the parameter space for the left oriented Fourier transform $\tilde{\mathcal{F}}_L(\tilde{q}_L)$ of function $\mathcal{F}(q)$ in equations (1) and (6).

$$\widetilde{\mathfrak{R}}_L = |\tilde{q}_L\rangle \tilde{q}_L \langle \tilde{q}_L| \tag{8}$$

Similarly the right oriented Fourier transform can be defined.

$$\tilde{\mathcal{F}}_R(\tilde{q}) = \int_q \mathcal{F}(q')\langle q'|\tilde{q}\rangle \; dq' \tag{9}$$

The reverse transform is:

$$\mathcal{F}(q) = \int_{\tilde{q}_R} \tilde{\mathcal{F}}_R(\tilde{q}_R)\langle q|\tilde{q}_R\rangle \, d\tilde{q}_R = \int_{\tilde{q}_R}\int_{q'} \mathcal{F}(q')\langle q'|\tilde{q}_R\rangle\langle \tilde{q}_R|q\rangle \, dq' \, d\tilde{q}_R \tag{10}$$

$$= \int_{q'} \mathcal{F}(q') \left\{ \int_{\tilde{q}_R} \langle q'|\tilde{q}_R\rangle\langle\tilde{q}_R|q\rangle \; d\tilde{q}_R \right\} dq' = \int_{q'} \mathcal{F}(q') \; \delta(q - q') \; dq'$$

Also here the functions $\langle q|q'\rangle$, $\langle\tilde{q}_R|\tilde{q}'_R\rangle$, $\langle\tilde{q}_R|q\rangle$ and $\langle q|\tilde{q}_R\rangle$ form sets of mutually orthogonal functions.

The reverse bra-ket form of the operator $\tilde{\mathcal{F}}_R$ equals:

$$\tilde{\mathcal{F}}_R = |\tilde{q}_R\rangle\tilde{\mathcal{F}}_R(\tilde{q}_R)\langle\tilde{q}_R| \tag{11}$$

Operator $\widetilde{\Re}_R$ provides the parameter space for the right oriented Fourier transform $\tilde{\mathcal{F}}_R(\tilde{q}_R)$ of function $\mathcal{F}(q)$ in equations (9) and (10).

$$\widetilde{\Re}_R = |\tilde{q}_R\rangle\tilde{q}_R\langle\tilde{q}_R| \tag{12}$$

The third version of the Fourier transform is:

$$\tilde{\mathcal{F}}(\tilde{q}_L, \tilde{q}_R) = \frac{\tilde{\mathcal{F}}_L(\tilde{q}_L) + \tilde{\mathcal{F}}_R(\tilde{q}_R)}{2} = ½ \int_q \{\langle\tilde{q}_L|q\rangle\mathcal{F}(q) + \mathcal{F}(q)\langle q|\tilde{q}_R\rangle\} \, dq \tag{13}$$

In contrast to the right and left version, the third version has no reverse.

3 Well-ordered reference operators

The eigenvalues of a normal operator T that resides in a separable Hilbert space can be ordered with respect to the real part of the eigenvalues. Operator $T_0 = (T + T^\dagger)/2$ is the corresponding self-adjoint operator. If each real value occurs only once, then the operator T and its adjoint $T^\dagger$ can be well-ordered. This means that the eigenvalues of T_0 are used as enumerators for other ordering processes. The imaginary part of the eigenvalues can then still be ordered in different ways. Operator $\boldsymbol{T} = (T - T^\dagger)/2$ is the corresponding anti-Hermitian operator. For example it can be ordered according to Cartesian coordinates or according to spherical coordinates. Also each of these orderings can be done in different ways.

The property of being well-ordered is restricted to operators with countable eigenspaces. However, via the defining functions, the well-orderedness can be transferred to the corresponding operator in the Gelfand triple.

3.1.1 Progression ordering

A single self-adjoint reference operator that offers an infinite set of rational eigenvalues can synchronize a ***category of well-ordered normal operators***. We use $\mathcal{R}_0$ for this purpose. The ordered eigenvalues of this self-adjoint operator act as progression values. In this way the infinite dimensional separable Hilbert space owns a ***model wide clock***. With this choice the separable Hilbert space steps with ***model-wide progression steps***.

The selected well-ordered normal reference operator $\mathcal{R}$ that resides in an infinite dimensional separable quaternionic Hilbert space is used in the specification of the companion quaternionic Gelfand triple. There it corresponds to reference operator $\mathfrak{R}$. In that way progression steps in the separable Hilbert space and flows in the companion Gelfand triple. Both reference operators will be used to provide parameter spaces.

The countable set of progression values of the Hermitian part $\mathcal{R}_0 = (\mathcal{R} + \mathcal{R}^\dagger)/2$ of the well-ordered reference operator $\mathcal{R}$ can be used to enumerate other ordered sequences.

3.1.2 Cartesian ordering

The whole separable Hilbert space can at the same time be spanned by the eigenvectors of a reference operator whose eigenvalues are well-ordered with respect to the real parts of the eigenvalues, while the imaginary parts are ordered with respect to a Cartesian coordinate system.

For Cartesian ordering, having an origin is not necessary. In ***affine Cartesian ordering*** only the direction of the ordering is relevant. Affine Cartesian ordering exists in eight symmetry flavors.

Cartesian ordering supposes a unique orientation of the Cartesian axes.

The well-ordered reference operator $\mathcal{R}$ is supposed to feature affine Cartesian ordering.

3.1.3 Spherical ordering

Spherical ordering starts with a selected Cartesian set of coordinates. In this case the origin is at a unique center location. Spherical ordering can be done by first ordering the azimuth and after that the polar angle is ordered. Finally, the radial distance from the center can be ordered. Another procedure is to start with the polar angle, then the azimuth and finally the radius. Such, spherical orderings may create a ***symmetry center***. Since the ordering starts with a selected Cartesian coordinate system, spherical ordering will go together with affine Cartesian ordering.

Each symmetry center is described by the eigenspaces of an anti-Hermitian operator $\mathfrak{S}_n^x$ that map a finite dimensional subspace of Hilbert space $\mathfrak{H}$ onto itself. Superscript ^{x} refers to the ordering type of the symmetry center. $\mathfrak{S}_n^x$ has no Hermitian part. Only through its ordering it can synchronize with progression steps. The subscript n enumerates the symmetry centers.

4 Symmetry flavor

Quaternions can be mapped to Cartesian coordinates along the orthonormal base vectors 1, $\boldsymbol{i}$, $\boldsymbol{j}$ and $\boldsymbol{k}$; with $\boldsymbol{ij} = \boldsymbol{k}$

Due to the four dimensions of quaternions, quaternionic number systems exist in 16 well-ordered versions $\{q^x\}$ that differ only in their discrete Cartesian symmetry set. The quaternionic number systems $\{q^x\}$ correspond to 16 versions $\{q_i^x\}$ of rational quaternions.

Half of these versions are right handed and the other half are left handed. Thus the handedness is influenced by the symmetry flavor.

The superscript ^{x} can be ⓪, ①, ②, ③, ④, ⑤, ⑥, ⑦, ⑧, ⑨, ⑩, ⑪, ⑫, ⑬, ⑭, or ⑮.

This superscript represents the ***symmetry flavor*** of the superscripted subject.

The reference operator $\mathcal{R}^{⓪} = \left|q_i^{⓪}\right\rangle q_i^{⓪} \left\langle q_i^{⓪}\right|$ in separable Hilbert space $\mathfrak{H}$ maps into the reference operator $\mathfrak{R}^{⓪} = \left|q^{⓪}\right\rangle q^{⓪} \left\langle q^{⓪}\right|$ in Gelfand triple $\mathcal{H}$.

The symmetry flavor of the symmetry center $\mathfrak{S}_n^x$, which is maintained by operator $\mathfrak{S}^x = |\mathfrak{s}_i^x\rangle \mathfrak{s}_i^x \langle \mathfrak{s}_i^x|$ is determined by its Cartesian ordering and then compared with the reference symmetry flavor, which is the symmetry flavor of the reference operator $\mathcal{R}^{⓪}$. ⬆⬆⬆⬆

Now the symmetry related charge follows in three steps.

1. Count the difference of the spatial part of the symmetry flavor of $\mathfrak{S}^x$ with the spatial part of the symmetry flavor of reference operator $\mathcal{R}^{⓪}$.
2. If the handedness changes from **R** to **L**, then switch the sign of the count.
3. Switch the sign of the result for anti-particles.

Electric charge equals symmetry related charge divided by 3.

Symmetry flavor					
Ordering x y z τ	Super script	Handedness Right/Left	Color charge	Electric charge * 3	Symmetry center type. Names are taken from the standard model
⬆⬆⬆⬆	⓪	**R**	N	+0	neutrino
⬇⬆⬆⬆	①	**L**	R	−1	down quark
⬆⬇⬆⬆	②	**L**	G	−1	down quark
⬇⬇⬆⬆	③	**L**	B	−1	down quark
⬆⬆⬇⬆	④	**R**	B	+2	up quark
⬇⬆⬇⬆	⑤	**R**	G	+2	up quark
⬆⬇⬇⬆	⑥	**R**	R	+2	up quark
⬇⬇⬇⬆	⑦	**L**	N	−3	electron
⬆⬆⬆⬇	⑧	**R**	N	+3	positron
⬇⬆⬆⬇	⑨	**L**	$\bar{R}$	−2	anti-up quark
⬆⬇⬆⬇	⑩	**L**	$\bar{G}$	−2	anti-up quark
⬇⬇⬆⬇	⑪	**L**	$\bar{B}$	−2	anti-up quark
⬆⬆⬇⬇	⑫	**R**	$\bar{B}$	+1	anti-down quark
⬇⬆⬇⬇	⑬	**R**	$\bar{R}$	+1	anti-down quark
⬆⬇⬇⬇	⑭	**R**	$\bar{G}$	+1	anti-down quark
⬇⬇⬇⬇	⑮	**L**	N	−0	anti-neutrino

Per definition, members of coherent sets $\{a_i^x\}$ of quaternions all feature the same symmetry flavor that is marked by superscript ^{x}.

Also continuous functions and continuums feature a symmetry flavor. Continuous quaternionic functions $\psi^x(q^x)$ and corresponding continuums do not switch to other symmetry flavors ^{y}.

The reference symmetry flavor $\psi^y(q^y)$ of a continuous function $\psi^x(q^y)$ is the symmetry flavor of the parameter space $\{q^y\}$.

The symmetry related charge conforms to the amount of reordering that is required when the symmetry center or one of its elements is mapped onto the reference space $\mathcal{R}^{⓪}$.

The concept of symmetry flavor sins against the cosmologic principle, which states that universe does not contain specific directions. It also claims that universe has no origin. Affine Cartesian ordering does not apply a selected spatial origin. That does not say that universe cannot have a unique spatial origin. That origin would be the spatial origin of reference operator $\mathcal{R}^{⓪}$. All symmetry centers own a unique spatial origin. That origin maps onto a dynamic location in $\mathcal{R}^{⓪}$.

5 Symmetry centers

Each symmetry center corresponds to a dedicated subspace of the infinite dimensional separable Hilbert space. That subspace is spanned by the eigenvectors $\{|\mathfrak{s}_i^x\rangle\}$ of a corresponding symmetry center reference operator $\mathfrak{S}_n^x$. Here the superscript ^{x} refers to the type of the symmetry center. The type covers more than just the symmetry flavor.

Symmetry flavors relate to affine Cartesian ordering. Each symmetry center will own a single symmetry flavor. The symmetry flavor of the symmetry center relates to the Cartesian coordinate system that acts as start for the spherical ordering. The combination of affine Cartesian ordering and spherical ordering puts corresponding axes in parallel. Spherical ordering relates to spherical coordinates. Starting spherical ordering with the azimuth corresponds to ***half integer spin***. The azimuth runs from 0 to π radians. Starting spherical ordering with the polar angle corresponds to ***integer spin***. The polar angle runs from 0 to 2π radians. These selections add to the type properties of the symmetry centers.

The model suggests that symmetry centers $\{\mathfrak{S}_n^x\}$ are maintained by special mechanisms $\{\mathfrak{M}_n\}$ that ensure the spatial and dynamical coherence of the coupling of the symmetry center to the background space. Several types of such mechanisms exist. Each symmetry center type corresponds to a class of mechanism types. ***These mechanisms are not part of the separable Hilbert space***.

Symmetry centers $\{\mathfrak{S}_n^x\}$ are ***resources*** where the coherence ensuring mechanisms $\{\mathfrak{M}_n\}$ can dynamically take locations that are stored in quaternionic eigenvalues of dedicated stochastic operators, in order to generate coherent location swarms that represent point-like objects. The type of the point-like object corresponds to the type of the controlling mechanism. The coherent location swarm corresponds with the eigenspace of the stochastic operator.

The basic symmetry center $\mathfrak{S}_n^x$ is independent of progression. Once created, a symmetry center persists until it is annihilated. However, during creation its ordering can be synchronized with selected progression steps. Any progression dependence that concerns a symmetry center $\mathfrak{S}_n^x$ is handled by a type dependent mechanism $\mathfrak{M}_n$. The type depends on the symmetry flavor and on the spin. Further, it depends on other characteristics that will appear as properties of the point-like object that will be supported by the controlling mechanism. An example is the generation flavor of the point-like particle. In this way the same symmetry center type can support electrons, muons and tau particles. Symmetry flavor and spin can be related to the ordering of the symmetry center $\mathfrak{S}_n^x$. Generation flavor is a property of the controlling mechanism $\mathfrak{M}_n$.

The mechanisms that control the usage of symmetry centers act mostly in a cyclic fashion. When compared to mechanisms that care about particles, the cycles that occur in equivalent mechanisms that care about corresponding anti-particles act in the reverse direction. As a consequence many of the properties of the anti-particles are the opposite of the properties of the corresponding particles. This holds for the sign of the symmetry related charge and it holds for the color charge, but it does not hold for the mass and for the energy of the (anti)particle.

Symmetry centers have a well-defined spatial origin. That origin floats on the eigenspace of the reference operator $\mathcal{R}^{⓪}$. Symmetry centers are formed by a dedicated category of ***compact anti-Hermitian operators*** $\{\mathfrak{S}_n^x\}$.

An infinite dimensional separable Hilbert space can house a huge but finite set of subspaces that each represent such a symmetry center. Each of these subspaces then corresponds to a dedicated spherically ordered reference operator $\mathfrak{S}_n^x$. The superscript ^{x} distinguishes between symmetry

flavors and other properties, such as spin and generation flavor. Symmetry centers correspond to dedicated subspaces that are spanned by the eigenvectors $\{|\mathfrak{s}_i^x\rangle\}$ of the symmetry center reference operator $\mathfrak{S}^x$.

$$\mathfrak{S}^x = |\mathfrak{s}_i^x\rangle \mathfrak{s}_i^x \langle \mathfrak{s}_i^x| \tag{1}$$

$$\mathfrak{S}^{x\dagger} = -\mathfrak{S}^x \tag{2}$$

Here we omitted subscript n.

Only the location of the center inside the eigenspace of reference operator $\mathcal{R}^{⓪}$ is a progression dependent value. This value is not eigenvalue of operator $\mathfrak{S}_n^x$. The location of the center inside $\mathcal{R}^{⓪}$ is eigenvalue of a central governance operator $\mathcal{g}$.

Symmetry centers feature a ***symmetry related charge*** that depends on the difference between the symmetry flavor of the symmetry center and the symmetry flavor of the reference operator $\mathcal{R}^{⓪}$, which equals the symmetry flavor of the embedding continuum $\mathfrak{C}$. The symmetry related charges raise a ***symmetry related field*** $\mathfrak{A}$. The symmetry related field $\mathfrak{A}$ influences the position of the center of the symmetry center in parameter space $\mathcal{R}^{⓪}$ and indirectly it influences the position of the map of the symmetry center into the field that represents the embedding continuum $\mathfrak{C}$. Both fields, $\mathfrak{A}$ and $\mathfrak{C}$ use the eigenspace of the reference operator $\mathfrak{R}$ as their parameter space.

The closed subspaces that correspond to a symmetry center have a fixed finite dimension. This dimension is the same for all types of symmetry centers. This ensures that symmetry related charges all appear in the same short list.

5.1 Synchronization via coupling

The basic symmetry center $\mathfrak{S}_n^x$ is independent of progression. Any progression dependence that concerns a symmetry center is handled by a type dependent mechanism $\mathfrak{M}_n$ that controls the usage of the symmetry center. The type dependent mechanism $\mathfrak{M}_n$ acts in a progression dependent fashion. On certain progression steps the mechanism selects a location from the symmetry center that will be used to embed a point-like object in the background space. The mechanism $\mathfrak{M}_n$ selects locations in accordance to the Poisson equation. If this is a screened Poisson equation, then that equation defines a clock signal with frequency ω, which can aid in the synchronization.

$$\langle \boldsymbol{\nabla}, \boldsymbol{\nabla} \rangle \chi - \omega^2 \chi = \rho \tag{1}$$

$$\chi = a(\boldsymbol{x}) \exp(\pm i\, \omega\, \tau) \tag{2}$$

The background space, is maintained by reference operator $\mathcal{R}^{⓪}$. Embedding the symmetry center into the eigenspace of this operator ensures the synchronization of the symmetry center with the

background space. That is why the embedding occurs at instances that are selected from the progression values, which are offered as eigenvalues by $\mathcal{R}_0^{\textcircled{0}} = \left(\mathcal{R}^{\textcircled{0}} + \mathcal{R}^{\textcircled{0}^\dagger}\right)/2$. However, the controlling mechanism $\mathfrak{M}_n$ does not embed the center location, but instead the mechanism $\mathfrak{M}_n$ uses a stochastic process in order to select a location somewhere inside the symmetry center. Further, not all eigenvalues $\{\mathfrak{s}_i^x\}$ of $\mathfrak{S}^x$ will be used in the embedding process. A special operator $\mathcal{o}^x$ that is dedicated to the type of the embedded point-like object describes the selected locations in its eigenvalues.

Eigenvalue a_i^x of operator $\mathcal{o}^x$ corresponds to a mapped eigenvalue $b_i^{\textcircled{0}}$ of operator $\mathcal{b}^{\textcircled{0}}$ in background space $\mathcal{R}^{\textcircled{0}}$. Since $\mathcal{R}^{\textcircled{0}}$ maps onto $\mathfrak{R}^{\textcircled{0}}$, the operator $\mathcal{b}^{\textcircled{0}}$ has an equivalent in the Gelfand triple. These maps are the result of a relocation of the whole location swarm $\{a_i^x\}$, which is due to the independent location and movement of the symmetry center. Due to the differences in symmetry flavor between the symmetry center and background space $\mathcal{R}^{\textcircled{0}}$, this map involves reordering of the spatial parts of the eigenvalues. Function $\mathfrak{C}(q)$maps the relocated swarm elements onto continuum $\mathfrak{C}$. Thus, operator $\mathcal{b}^{\textcircled{0}}$ has images $\mathcal{b}^{\textcircled{0}}$ and $\mathfrak{C}(\mathcal{b}^{\textcircled{0}})$ in the Gelfand triple.

The final embedding location of swarm element a_i^x represents a point-like object that originally resided in the symmetry center. That embedding location is mapped onto the embedding continuum, which resides as the eigenspace of operator $\mathfrak{C}$ in the Gelfand triple $\mathcal{H}$. This continuum is defined as a function $\mathfrak{C}(q)$ over parameter space $\mathfrak{R}^{\textcircled{0}}$.

The locations in the symmetry center that for the purpose of the embedding are selected, form a coherent location swarm and a hopping path that together characterize the dynamic behavior of the point-like object. The embedding process deforms continuum $\mathfrak{C}$. It does not affect the parameter spaces $\mathcal{R}^{\textcircled{0}}$ and $\mathfrak{R}^{\textcircled{0}}$. This embedding process is treated in more detail in section 11; Embedding.

5.2 Hadronic centers

Symmetry centers can bind into hadronic centers that feature isotropic symmetry. In reverse the hadronic centers can split into symmetry centers.

Hadronic centers feature zero or full symmetry related charge. Hadronic centers exist as meson centers and as baryon centers.

5.2.1 Baryon centers

Baryon centers are governed by tri-state switchers, which govern the states of three quarks and join them into a colorless union.

5.2.2 Meson centers

Meson centers are colorless combinations of quarks and anti-quarks.

6 Central governance

The eigenvalues $\mathcal{g}(q,n)$ of the central governance operator $\mathcal{g}$ administer the relative locations of the symmetry centers $\mathfrak{S}_n^x$ with respect to the reference operator $\mathcal{R}^{⓪}$ which resides in the separable Hilbert space $\mathfrak{H}$ and maps to the reference continuum $\mathfrak{R}^{⓪}$ in the Gelfand triple $\mathcal{H}$. A further map projects onto the embedding continuum $\mathfrak{C}$.The central governance operator $\mathcal{g}$ resides in the separable Hilbert space $\mathfrak{H}$. Operator $\mathcal{g}$ has an equivalent $\mathfrak{C}(\mathcal{g})$ in the Gelfand triple. Function $\mathfrak{C}(q)$ maps eigenvalues $\mathcal{g}(q,n)$ of $\mathcal{g}$ onto continuum $\mathfrak{C}$.

The reference continuum $\mathfrak{R}^{⓪}$ acts as a parameter space of the function $\mathfrak{A}(q)$ that specifies the symmetry related field $\mathfrak{A}$, which is eigenspace of the corresponding operator.

Each symmetry center owns a symmetry related charge, which is located at its geometric center. Each symmetry related charge owns an individual field φ that contributes to the overall symmetry related field $\mathfrak{A}$.

The reference continuum $\mathfrak{R}^{⓪}$ also acts as a parameter space of the function $\mathfrak{C}(q)$ that specifies the embedding continuum $\mathfrak{C}$, which is eigenspace of the corresponding operator $\mathfrak{C}$.

A fundamental difference exists between field $\mathfrak{A}$ and field $\mathfrak{C}$. However, both fields obey the same quaternionic differential calculus. The difference originates from the kind of artifacts that cause the discontinuities of the fields. In the symmetry related field $\mathfrak{A}$ these artifacts are the symmetry related charges. In the embedding continuum $\mathfrak{C}$ these artifacts are the embedding events. What happens in not too violent conditions and in not too wide ranges will be described by the second order partial differential equation of the corresponding field and will be affected by the local and current conditions. Since the elementary point-like objects reside inside their individual symmetry center, the embedding continuum will also be affected by what happens to the symmetry centers.

Double differentiation of field $\mathfrak{A}$ shows the relation between $\mathfrak{A}$ and $\mathcal{g}$.

$$\nabla^* \nabla \, \mathfrak{A} = \mathcal{g} \tag{1}$$

6.1 Embedding symmetry centers

The well-ordered eigenspace of a quaternionic normal operator $\mathcal{R}^{⓪}$ that resides in an infinite dimensional separable Hilbert space acts as a reference operator from which the parameter space $\mathfrak{R}^{⓪}$ of the embedding continuum $\mathfrak{C}$ will be derived. This parameter space resides as continuum eigenspace of a corresponding operator $\mathfrak{R}^{⓪}$ in the Gelfand triple. This parameter space also acts as parameter space of a symmetry related field $\mathfrak{A}$. It is sparsely covered by locations of symmetry centers. The central governance operator $\mathcal{g}$ administers these locations. The symmetry centers contain symmetry related charges. The locations of these charges are influenced by the symmetry related field $\mathfrak{A}$. Function $\mathfrak{C}(q)$ maps both φ and the eigenspace of $\mathcal{g}$ onto continuum $\mathfrak{C}$.

7 Modules

Modules are represented by closed subspaces of the separable Hilbert space, but not every closed subspace represents a module or modular system. In fact only a small minority of the closed subspaces will act as actual modules. What renders a closed subspace into a module and what combines modules into subsystems or systems? The answers to these questions can only be found by investigating the contents of the closed subspaces.

A special category of modules are ***elementary modules***. Elementary modules are not constituted of other modules. They are the atoms of the orthomodular lattice, which describes the relations between modules and modular systems. All elementary modules reside on a their own individual symmetry center.

7.1 Module content

In free translation, the spectral theorem for normal operators that reside in a separable Hilbert space states: "If a normal operator maps a closed subspace onto itself, then the subspace is spanned by an orthonormal base consisting of eigenvectors of the operator." The corresponding eigenvalues characterize this closed subspace.

It is possible to select a quaternionic normal operator for which a subset of the eigenvectors span the closed subspace and the corresponding eigenvalues describe the dynamic geometric data of this module. By ordering the real values of these eigenvalues, the geometric data become functions of what we will call ***progression***.

7.1.1 Progression window

Here we only consider elementary modules for which the content is ***well-ordered***. This means that every progression value is only used once.

For the most primitive modules the closed subspace may be reduced until it covers a generation cycle in which the statistically averaged characteristics of the module mature to fixed values. The resulting closed subspace acts as a ***sliding progression window***.

The sliding window separates a deterministic history from a partly uncertain future. Inside the sliding window ***a dedicated mechanism*** $\mathfrak{M}_n$ ***fills the eigenspace*** of stochastic operator $\mathcal{O} = |a_j\rangle a_j \langle a_j|$. The mechanism is a function of progression. If it is a cyclic function of progression, then the module is recurrently regenerated.

7.2 Symmetry center as platform

All elementary modules are supposed to reside in an individual symmetry center. However, at every progression instant the elementary module occupies only one location of the symmetry center. During the regeneration cycle of the module the occupied locations form a coherent location swarm and at the same time the locations form a hopping path. Symmetry centers float on an embedding medium. That embedding continuum corresponds to a well-ordered normal reference operator, whose eigenvectors span the whole infinite dimensional separable Hilbert space.

7.3 Map into a continuum

By imaging the discrete eigenvalues into a reference space, the discrete eigenvalues form a ***swarm*** $\{a_j^x\}$, which is a subset of the rational quaternions $\{\mathbf{s}_i^x\}$ that form the symmetry center on which the module resides. At the same time the discrete eigenvalues form a ***hopping path***. With other words the swarm forms a spatial map of the dynamic hopping of the point-like object. The swarm and the

hopping path conform to a stochastic operator σ^x that is well ordered with respect to its progression values, but is not ordered in spatial sense like reference operators $\mathcal{R}$ or $\mathfrak{S}_n^x$.

$$\sigma^x = \left|a_j^x\right\rangle a_j^x \left\langle a_j^x\right|$$

This temporal ordering is installed via the quaternionic version of the screened Poisson equation. That equation involves a symmetry center wide clock that can synchronize the location generation process with the model wide progression steps that are oppressed by reference operator $\mathcal{R}^{⓪}$.

Next, we use a map $\mathcal{M}_1$ of the swarm into the reference continuum that is the eigenspace of the reference operator $\mathfrak{R}^{⓪}$. This operator and its eigenspace reside in the Gelfand triple $\mathcal{H}$.

In the model, two maps $\mathcal{M}_1$ and $\mathcal{M}_2$ are relevant. The first map $\mathcal{M}_1$ has the flat reference continuum $\mathfrak{R}^{⓪} = \{q^{⓪}\}$ as target. ***This reference continuum is not affected by the imaging***. Only the locations of the symmetry centers are affected by the influence of the symmetry related field $\mathfrak{A}$. The second map $\mathcal{M}_2$ has the deformable continuum $\mathfrak{C}$ as target. In contrast, $\mathfrak{C}$ ***is affected by the embedding process***.

In the symmetry center the hopping path is closed. If the image of the hopping path is also closed in the reference continuum $\mathfrak{R}^{⓪}$, then the swarm stays at the same location in the map $\mathcal{M}_1$ onto the reference continuum $\mathfrak{R}^{⓪}$. This does not need to be the case for the map $\mathcal{M}_2$ into the embedding continuum $\mathfrak{C}$. The two target continuums $\mathfrak{R}$ and $\mathfrak{C}$ reside as eigenspaces in the Gelfand triple.

We will interpret the two maps to work in succession. The second map $\mathcal{M}_2$ maps the reference continuum $\mathfrak{R}^{⓪}$ that resides in the Gelfand triple into the embedding continuum $\mathfrak{C}$, which also resides in the Gelfand triple.

7.4 Coherent elementary modules

Coherent elementary modules are directly related to a symmetry center. The elements of the coherent location swarm that characterizes the coherent elementary module are taken from the symmetry center. These elements are ordered with respect to progression, but spatially they are selected in a stochastic fashion. This selection is described by operator σ^x. In the map onto the reference continuum, coherent elementary modules feature a hopping path. Inside the symmetry center the hopping path is closed. Further, for coherent elementary modules, the map of the location swarm into the reference continuum corresponds to an operator ρ that is defined by a continuous function. That continuous function is a ***normalized location density distribution*** and it has a ***Fourier transform***. As a consequence the operator that conforms to this function has a different ordering with respect to its spatial values. That new operator ρ has $\mathcal{R}$ as its parameter space. It tends to describe the swarm as a whole unit. It no longer describes the hopping path.

Coherence is ensured by a mechanism $\mathfrak{M}_n$ *that selects the eigenvalues such that a coherent swarm is generated*.

The notion of ***coherent swarm*** will be defined later. Coherent elementary modules are characterized by the symmetry flavor of their symmetry center $\mathfrak{S}_n^x$. When mapped into a reference continuum that is eigenspace of reference operator $\mathfrak{R}^{⓪} = \left|q^{⓪}\right\rangle q^{⓪} \left\langle q^{⓪}\right|$ the module is characterized by a ***symmetry related charge***, which is *located at the center of symmetry*. The symmetry related charge is a property of the local ***symmetry center*** $\mathfrak{S}_n^x$.

The size and the sign of the symmetry related charge depends on the difference of the symmetry flavor of the local symmetry center with respect to the symmetry flavor of the reference continuum $\mathcal{R}^{⓪}$. The coherent swarm $\{a_j^x\}$ inherits the symmetry flavor of the local symmetry center $\mathfrak{S}_n^x$.

However, the controlling mechanism $\mathfrak{M}_n$ picks the elements of this set in a spatially stochastic way instead of in a spatially ordered fashion. Thus the operator σ^xthat reflects the stochastic selection, corresponds with another operator ρ^x that reflects the spatial ordering and supports the coherent stochastic mechanism $\mathfrak{M}_n$ in achieving spatial coherence.

7.5 The function of coherence

Embedding of point-like objects into the affected embedding continuum spreads the reach of the separate embedding locations and offers the possibility to bind modules. The spread of the embedded point-like object is defined by the Green's function of the non-homogeneous second order partial differential equation. However, spurious embedding locations have not enough strength and not enough reach to implement an efficient binding effect. In contrast, coherent location swarms offer enough locality and enough strength in order to bind two coherent swarms that are sufficiently close.

For example a Gaussian distribution of the location swarm would turn the very peaky Green's function into a rather broad spherical painting brush that can be described by the potential:

$$\varphi(r) = \frac{ERF(r)}{r}$$

This is a smooth function without a trace of a singularity.

Imaging of the location swarm into the reference continuum is only used to define coherence and to indicate the influence of the symmetry related charges. The embedding into the affected continuum is used to exploit the corresponding potential binding effect of the swarm.

8 The orthomodular base model

We have achieved a level in which the major chain of mathematical structures does no longer offer an inescapable self-evident extension. The model uses separable and non-separable Hilbert spaces in order to store numeric data that can describe a series of discrete objects that are embedded in a continuum. The real parts of the parameters can be used to order the parameters and the target values of functions. If properly ordered these descriptions can represent a sequence of static status quos. However, this model contains no means to control the ***coherence*** between the subsequent members of the sequence.

We will call this stage of the model development "***The orthomodular base model***". Any further development of the model involves the insertion of mechanisms that ensure the coherence between the subsequent members of the sequence of static status quos.

The orthomodular base model describes the relational structure of modular systems. Via the management mechanisms it can add characteristics to the modules. These characteristics are based on eigenvalues of normal operators that reside in the separable Hilbert space and have eigenvectors in the closed subspace that represents the module. The Hilbert spaces only support storage and description. The management mechanisms represent the actual drivers of the model.

The numeric data that occur in the orthonormal base model must be taken from division rings. The most elaborate choice for these data are quaternions.

Quaternions and Hilbert spaces can represent a wider usage than just the storage of dynamic geometric data. Quaternions can implement rotations. In this way they can shift properties between dimensions. This is shown in section 20; Tri-state spaces.

The peculiarities of these quaternions influence the features and the behavior of the discrete objects and the fields that occur in the orthonormal model. Many of these peculiarities are hardly known by scientists. As far as they apply to this paper these subjects are treated in the Appendix.

Concepts such as symmetry centers and coherent location swarms are not part of the orthonormal base model, but these features make use of the structure and the properties of the orthonormal base model. The same holds for the symmetry related field $\mathfrak{A}$ and the embedding continuum $\mathfrak{C}$. However, the reference operators that can be applied as parameter spaces can be considered as standard properties of quaternionic Hilbert spaces. They can be considered to belong to the orthomodular base model.

9 Fields

A category of operators can represent quaternionic functions. This is applicable both in the separable Hilbert space and in the Gelfand triple.

In this paper, fields are continuums that are target spaces of quaternionic functions that define eigenspaces of operators, which reside in the Gelfand triple.

Quaternionic functions and their differentials can be split in a real scalar functions and imaginary vector functions. Here we will only consider not too violent disruptions of the continuity of the fields. We also restrict the validity range of the equations. With these restrictions the quaternionic nabla can be applied and the discontinuities restrict to point-like artifacts..

Quaternionic functions can represent fields and continuums, but they can also represent density distributions of discrete dynamic locations. Quaternionic differentiation is treated in the next chapter and in the appendix.

Double differentiation of a basic field leads to a non-homogeneous second order partial differential equation that relates the basic field to the corresponding density distributions of discrete dynamic locations of the artifacts that cause the local discontinuities of the basic field.

The symmetry related field $\mathfrak{A}$ and the embedding continuum $\mathfrak{C}$ are basic fields.

The symmetry related field $\mathfrak{A}$ is based on the existence of symmetry centers. These symmetry centers float over a background reference space.

The embedding continuum $\mathfrak{C}$ is based on the existence of a dynamic deformable function that describes the embedding of discrete artifacts, which reside on symmetry centers and are mapped onto $\mathfrak{C}$. The artifacts are selected by a mechanism $\mathfrak{M}_n$ that is dedicated to the symmetry center $\mathfrak{S}_n^x$. The acts of these mechanisms can be described by a corresponding stochastic operator.

9.1 Subspace maps

The orthomodular base model consist of two related Hilbert spaces.

- A separable Hilbert space $\mathfrak{H}$ that acts as a descriptor of the properties of all discrete objects.
- A non-separable Hilbert space $\mathcal{H}$ that acts as a descriptor of the properties of all continuums.
    - This non-separable Hilbert space embeds its companion separable Hilbert space $\mathfrak{H}$.

The two Hilbert spaces are coupled by the well-ordered reference operator $\mathcal{R}^{⓪}$ and the corresponding reference operator $\mathfrak{R}^{⓪}$. Both are defined by the quaternionic function $\mathfrak{R}(q) \equiv q$.

Controlling mechanisms $\{\mathfrak{M}_n\}$ fill the module related subspaces of separable Hilbert space $\mathfrak{H}$ with data and the contents of these subspaces are subsequently embedded into the non-separable Hilbert space $\mathcal{H}$. The fill of subspaces with data is described by dedicated stochastic operators. The mechanisms $\{\mathfrak{M}_n\}$ use stochastic processes in order to generate these data.

A closed subspace in $\mathfrak{H}$ maps into a subspace of $\mathcal{H}$. Only countable subspaces of $\mathcal{H}$ have a sensible dimension. Defining functions can map countable eigenspaces in the separable Hilbert space into continuum eigenspaces in the Gelfand triple. Mapping does not influence the flat reference fields that are in use as parameter spaces.

9.2 Parameter spaces

The reference operator $\mathfrak{R}^{⓪}$ that reside in the Gelfand triple delivers a simple field that can act as a flat parameter space. This field is not affected by the embedding map. Via its defining function $\mathfrak{R}^{⓪}\left(q^{⓪}\right) = q^{⓪}$, it is a direct map of parameter space $\mathcal{R}^{⓪}$.

Symmetry centers are spanned by the eigenvectors $\{|\mathfrak{s}_i^x\rangle\}$ of a compact symmetry center reference operator $\mathfrak{S}_n^x$. The superscript ^{x} distinguishes between properties such as symmetry flavors and spin. Symmetry centers are special forms of parameter spaces that reside in the separable Hilbert space $\mathfrak{H}$. They also have a representation in the Gelfand triple. In the separable Hilbert space $\mathfrak{H}$ they have a fixed finite dimension, which is the same for all symmetry centers. Reference operator $\mathfrak{R}^{⓪}$ acts as the playground of maps of symmetry centers that define local symmetry related charges. Symmetry centers float over this background space.

9.3 Embedding field

The elements of the eigenspace of the stochastic operator $\mathscr{o}$, which is used by a controlling mechanism $\mathfrak{M}_n$ will be embedded in the eigenspace of operator $\mathfrak{C}$. This eigenspace is deformable and resides in the Gelfand triple $\mathcal{H}$. The stochastic operator resides in the separable Hilbert space $\mathfrak{H}$. It is connected to an elementary module and its controlling mechanism $\mathfrak{M}_n$ picks the eigenvalues of this operator from a corresponding symmetry center. These eigenvalues are mapped to parameter spaces $\mathfrak{R}^{⓪}$ and $\mathfrak{R}^{⓪}$. This converts operator $\mathscr{o}$ to operator $\mathscr{b}$. Operator $\mathscr{o}$ resides in separable Hilbert space $\mathfrak{H}$. Operator $\mathscr{b}$ resides both in the separable Hilbert space and in Gelfand triple $\mathcal{H}$. The map involves a shift of the locations of the swarm elements.

Operator $\mathfrak{C}$ can be described by a quaternionic function $\mathfrak{C}(q^{⓪})$ that has a parameter space, which is generated by the eigenspace of operator $\mathfrak{R}^{⓪}$. The embedding process can be described by quaternionic differential calculus. If the discontinuities that are generated by local discontinuities are not too violent , then the non-homogeneous second order partial differential equation will elucidate the embedding process.

We will show that two different non-homogeneous second order partial differential equations exist that offer different views on the embedding process. The quaternionic differential calculus cannot show wave behavior. However, the Maxwell based differential calculus offers a non-homogeneous second order partial differential equation, which is also a second order partial differential equation.

In $\mathcal{H}$the operator $\mathfrak{C} = \left|q^{⓪}\right\rangle\mathfrak{C}\left(q^{⓪}\right)\left\langle q^{⓪}\right|$ is defined by function $\mathfrak{C}\left(q^{⓪}\right)$ and represents an embedding continuum $\mathfrak{C}$. This continuum gets affected by the embedding process and thus deforms dynamically.

The embedding continuum is always and everywhere present. It is deformed and vibrated by discrete artifacts that are embedded in this field.

In $\mathcal{H}$, the representations of symmetry centers float over the parameter space $\mathfrak{R}^{⓪}$ of the embedding continuum. The symmetry related charges of the symmetry centers generate local contributions to the symmetry related field $\mathfrak{A}$. The location of the center of the symmetry center within parameter space $\mathfrak{R}^{⓪}$ is affected by the symmetry related field $\mathfrak{A}$.

The mechanism $\mathfrak{M}_n$ that controls stochastic operator $\mathscr{o}$ picks members of a symmetry center and stores them in the eigenvalues of that operator. These eigenvalues are mapped to parameter space $\mathcal{R}^{⓪}$ and become eigenvalues of a new operator $\mathscr{b}$. This map involves relocation and re-ordering. This fact couples the location of the symmetry related charge of this symmetry center

with the locations that get embedded in the eigenspace of operator $\mathfrak{C}$. However, the parameter location of the symmetry related charge does not coincide with the parameter location of the eigenvalue of operator $\mathscr{b}$,that will be embedded in the eigenspace of operator $\mathfrak{C}$. This embedding involves a map that is described by function $\mathfrak{C}(\mathrm{q})$. The eigenvalues of operator $\mathscr{b}$ will form a swarm whose center will coincide with the parameter location of the symmetry related charge. That location also coincides with the location of the geometric center of the symmetry center. This location is not embedded and therefore it does not deform the eigenspace of operator $\mathfrak{C}$.

9.4 Symmetry related fields

Due to their four dimensions, quaternionic number systems exist in sixteen versions that only differ in their symmetry flavor. The elements of coherent sets of quaternions belong to the same symmetry flavor. This is the symmetry flavor of the symmetry center that supports the original location swarm. Differences between symmetry flavors of a symmetry center and the symmetry flavor of the eigenspace of the surrounding reference operator $\mathcal{R}^{\textcircled{0}}$ cause the presence of a symmetry related charge at the center location of that symmetry center. The countable reference parameter space $\mathcal{R}^{\textcircled{0}}$ in the separable Hilbert space $\mathfrak{H}$ maps onto the continuum parameter space $\mathfrak{R}^{\textcircled{0}}$, which resides in the Gelfand triple $\mathcal{H}$.

Symmetry related charges are point-like objects. These charges ***generate a field*** $\mathfrak{A}$ that differs from the embedding continuum. This symmetry related field also plays a role in the binding of modules, but that role differs significantly from the role of the embedding continuum $\mathfrak{C}$. The defining function $\mathfrak{A}(q)$ of field $\mathfrak{A}$ and the defining function $\mathfrak{C}(\mathrm{q})$ of field $\mathfrak{C}$ use the same parameter space $\mathfrak{R}^{\textcircled{0}}$.

Symmetry related charges are located at the geometric centers of local symmetry centers. The size and the sign of the symmetry related charge depends on the difference of the symmetry flavor of the symmetry center with respect to the symmetry flavor of the embedding continuum. Symmetry centers that belong to different symmetry related charges appear to try to compensate the symmetry differences. Equally signed charges repel and differently signed charges attract. The attached coherent location sets that are attached to the symmetry centers will be affected by these effects.

The symmetry related field $\mathfrak{A}$ can affect the locations of the symmetry related charges in the first map $\mathcal{M}_1$. *This means that with the centers of symmetry also the corresponding coherent swarms are relocated.* This can be interpreted as if the symmetry related field $\mathfrak{A}$ acts as a deformed parameter space for the embedding continuum $\mathfrak{C}$. Here we ignore this possibility and consider $\mathfrak{R}^{\textcircled{0}}$ as the flat parameter space of $\mathfrak{C}$.

The symmetry related charges do not directly affect the embedding continuum $\mathfrak{C}$. Their effects are confined to map $\mathcal{M}_1$. However, with their action the symmetry related charges ***relocate*** the centers of the corresponding coherent swarms. The elements of the swarms deform the embedding continuum.

The symmetry related charges are point charges. As a consequence the range of the field that is generated by a single charge is rather limited. The corresponding Green's function diminishes as 1/r with distance r from the charge $\mathfrak{C}$.

Fields of point charges superpose. A wide spread uniform distribution of symmetry related point charges can generate a corresponding wide spread symmetry related field $\mathfrak{A}$. This works well if a majority of the charges have the same sign. Still, relevant values of the symmetry related field $\mathfrak{A}$ depend on the nearby existence of symmetry related charges.

Coherent swarms are recurrently regenerated on their symmetry centers. The symmetry centers are not recurrently generated, but instead they can get relocated. Together with these symmetry centers the corresponding symmetry related charges and the residing swarms get relocated.

9.5 Free space

In the separable Hilbert space, the eigenvectors of the well-ordered reference operator $\mathcal{R}^{⓪}$ that do not belong to a module subspace together span free space. The elementary modules reside on symmetry centers whose center locations float on the eigenspace of $\mathcal{R}^{⓪}$.

At every progression instant only one element of the swarm $\{a_j^x\}$ is used. Thus “free space” surrounds all elements of the swarm. It forms most of the continuum $\mathfrak{C}$, which is deformed by the embedding of the currently selected swarm element.

10 Field dynamics

10.1 Differentiation

In the model that we selected, the dynamics of the fields can be described by quaternionic differential calculus. Apart from the eigenspaces of reference operators and the symmetry centers we encountered two fields that are defined by quaternionic functions and corresponding operators. One is the symmetry related field $\mathfrak{A}$ and the other is the embedding field $\mathfrak{C}$.

$\mathfrak{A}$ determines the dynamics of the symmetry centers. $\mathfrak{C}$ gets deformed and vibrated by the recurrent embedding of point-like elementary particles that each reside on an individual symmetry center.

Apart from the way that they are affected by point-like artifacts that disrupt the continuity of the field, both fields obey, under not too violent conditions and over not too large ranges, the same differential calculus. However, especially field $\mathfrak{A}$ is known to show wave behavior that cannot properly be described by quaternionic differential calculus. For that reason we will also investigate what a change of parameter space brings for the defining functions of the basic fields $\mathfrak{A}$ and $\mathfrak{C}$.

Besides quaternionic differential calculus exists Maxwell based differential calculus. The Maxwell equations use coordinate time instead of pure progression as one of the four parameters. The other three parameters together form the spatial part of the Maxwell based parameter space. Coordinate time can be interpreted as quaternionic distance. As a consequence this new parameter space has a Minkowski signature, while the quaternionic parameter space has a Euclidean signature. This difference is reflected in the second order partial differential equations of the two approaches. The Maxwell based differentia calculus offers a wave equation, while the quaternionic differential calculus does not describe dynamic waves.

Let us introduce variables Δt and $\Delta r = |\Delta \boldsymbol{x}|$. In quaternionic differential calculus $\Delta t = \Delta\tau$. In Maxwell based differential calculus $\Delta t = |\Delta x|$. Here in quaternion space $\Delta x = \Delta\tau + \Delta \boldsymbol{x}$ is a full quaternion step.

10.2 Quaternionic differential calculus.

Under rather general conditions the change of a quaternionic function $f(q)$ can be described by:

$$df(q) \approx \sum_{\mu=0\ldots3} \left\{ \frac{\partial f}{\partial q_\mu} + \sum_{\mu=0\ldots3} \frac{\partial}{\partial \nu} \frac{\partial f}{\partial q_\mu} dq^\nu \right\} dq^\mu = c_\mu(q) dq^\mu + c_{\mu\nu}(q) dq^\mu dq^\nu \tag{1}$$

Here the coefficients $c^\mu(q)$ and $c_{\mu\nu}(q)$ are full quaternionic functions. dq^μ are real numbers. e^ν are quaternionic base vectors.

Under more moderate and sufficiently short range conditions the function behaves more linearly.

$$df(q) \approx \sum_{\mu=0\ldots3} \frac{\partial f}{\partial q_\mu} dq^\mu = c_\mu(q) dq^\mu \tag{2}$$

Under even stricter conditions the functions become real functions $c_0^\mu(q)$ attached to quaternionic base vectors:

$$df(q) = c_0^\tau \, dq_\tau + c_0^x \, \boldsymbol{i} \, dq_x + c_0^y \, \boldsymbol{j} \, dq_y + c_0^z \, \boldsymbol{k} \, dq_z = c_0^\mu(q) \, e_\mu \, dq_\mu \tag{3}$$

Thus, in a rather flat continuum we can use the quaternionic nabla ∇.

$$\nabla = \left\{\frac{\partial}{\partial\tau}, \frac{\partial}{\partial x}, \frac{\partial}{\partial y}, \frac{\partial}{\partial z}\right\} = \frac{\partial}{\partial\tau} + \boldsymbol{i}\frac{\partial}{\partial x} + \boldsymbol{j}\frac{\partial}{\partial y} + \boldsymbol{k}\frac{\partial}{\partial z} = \nabla_0 + \boldsymbol{\nabla} \tag{3}$$

$$\Phi = \Phi_0 + \boldsymbol{\Phi} = \nabla\psi = (\nabla_0 + \boldsymbol{\nabla})(\psi_0 + \boldsymbol{\psi}) \tag{4}$$

$$\Phi_0 = \nabla_0\psi_0 - \langle \boldsymbol{\nabla}, \boldsymbol{\psi} \rangle \tag{5}$$

$$\boldsymbol{\Phi} = \nabla_0\boldsymbol{\psi} + \boldsymbol{\nabla}\psi_0 \pm \boldsymbol{\nabla} \times \boldsymbol{\psi} \tag{6}$$

In this form the differential equations can still describe point-like disruptions of the continuity of the field.

Double differentiation will then result in the quaternionic non-homogeneous second order partial differentiation equation:

$$\xi = \xi_0 + \boldsymbol{\xi} = \nabla^*\nabla\psi = (\nabla_0 - \boldsymbol{\nabla})(\nabla_0 + \boldsymbol{\nabla})(\psi_0 + \boldsymbol{\psi}) = \{\nabla_0\nabla_0 + \langle \boldsymbol{\nabla}, \boldsymbol{\nabla} \rangle\}\psi \tag{7}$$
$$= \frac{\partial^2\psi}{\partial\tau^2} + \frac{\partial^2\psi}{\partial x^2} + \frac{\partial^2\psi}{\partial y^2} + \frac{\partial^2\psi}{\partial z^2}$$

Here ξ is a quaternionic function that for a part ρ describes the density distribution of a set of point-like artifacts that disrupt the continuity of function $\psi(q)$.

$$\rho = \rho_0 + \boldsymbol{\rho} = \langle \boldsymbol{\nabla}, \boldsymbol{\nabla} \rangle\psi = \frac{\partial^2\psi}{\partial x^2} + \frac{\partial^2\psi}{\partial y^2} + \frac{\partial^2\psi}{\partial z^2} \tag{8}$$

$$\xi - \rho = \nabla_0 \nabla_0 \psi \tag{9}$$

In case of a single static artifact, the solution ψ will describe the corresponding Green's function.

Function $\psi(q)$ describes the mostly continuous field ψ.

The second order partial differential equation can be split into two continuity equations:

$$\Phi = \nabla \psi \tag{10}$$

$$\rho = \nabla^* \Phi \tag{11}$$

If ψ and Φ are normalizable functions and $\|\psi\| = 1$, then with real m and $\|\zeta\| = 1$

$$\nabla \psi = m\, \zeta \tag{12}$$

10.3 Fourier equivalents

In this quaternionic differential calculus, differentiation is implemented as multiplication.

This is revealed by the Fourier equivalents of the equations (4) through (10) in the previous paragraph:

$$\tilde{\Phi} = \tilde{\Phi}_0 + \tilde{\boldsymbol{\Phi}} = p\, \tilde{\psi} = (p_0 + \boldsymbol{p})(\tilde{\psi}_0 + \tilde{\boldsymbol{\psi}}) \tag{1}$$

The nabla ∇ is replaced by operator p. $\tilde{\Phi}$ is the Fourier transform of Φ.

$$\tilde{\Phi}_0 = p_0 \tilde{\psi}_0 - \langle \boldsymbol{p}, \tilde{\boldsymbol{\psi}} \rangle \tag{2}$$

$$\tilde{\boldsymbol{\Phi}} = p_0 \tilde{\boldsymbol{\psi}} + \boldsymbol{p} \tilde{\psi}_0 \pm \boldsymbol{p} \times \tilde{\boldsymbol{\psi}} \tag{3}$$

The equivalent of the quaternionic second order partial differential equation is:

$$\tilde{\xi} = \tilde{\xi}_0 + \tilde{\boldsymbol{\xi}} = p^* p\, \tilde{\psi} = \{p_0 p_0 + \langle \boldsymbol{p}, \boldsymbol{p} \rangle\} \tilde{\psi} \tag{4}$$

$$\tilde{\rho} = \tilde{\rho}_0 + \tilde{\boldsymbol{\rho}} = \langle \boldsymbol{p}, \boldsymbol{p} \rangle \tilde{\psi} \tag{5}$$

The continuity equations result in:

$$\widetilde{\Phi} = p\tilde{\psi} \tag{6}$$

$$\tilde{\rho} = p^{*}\widetilde{\Phi} \tag{7}$$

10.4 Poisson equations

The screened Poisson equation is a special condition of the non-homogeneous second order partial differential equation in which some terms are zero or have a special value.

$$\nabla^{*}\nabla\psi = \nabla_0\nabla_0\psi + \langle\boldsymbol{\nabla},\boldsymbol{\nabla}\rangle\psi = \xi \tag{1}$$

$$\nabla_0\nabla_0\psi = -\lambda^2\,\psi = \xi - \rho \tag{2}$$

$$\langle\boldsymbol{\nabla},\boldsymbol{\nabla}\rangle\psi - \lambda^2\psi = \xi \tag{3}$$

The 3D solution of this equation is determined by the screened Green's function $G(r)$.

Green functions represent solutions for point sources.

$$G(r) = \frac{\exp(-\lambda\, r)}{r} \tag{4}$$

$$\psi = \iiint G(\boldsymbol{r} - \boldsymbol{r}')\,\rho(\boldsymbol{r}')\,d^3\boldsymbol{r}' \tag{5}$$

G(r) has the shape of the Yukawa potential [9]

In case of $\lambda = 0$ it resembles the Coulomb or gravitation potential of a point source.

If $\lambda \neq 0$, then a solution of equation (2) is:

$$\psi = a(\boldsymbol{x})\,\exp(\pm\, i\,\omega\,\tau);\, \lambda = \pm\, i\,\omega \tag{6}$$

10.5 Solutions of the homogeneous second order partial differential equation

Solutions of the quaternionic homogeneous second order partial differential equation are of special interest because for odd numbers of participating dimensions this equation has solutions in the form of shape keeping fronts.

This homogeneous partial differential equation is given by:

$$\nabla^*\nabla\psi = \nabla_0\nabla_0\psi + \langle\boldsymbol{\nabla},\boldsymbol{\nabla}\rangle\psi = \frac{\partial^2\psi}{\partial\tau^2} + \frac{\partial^2\psi}{\partial x^2} + \frac{\partial^2\psi}{\partial y^2} + \frac{\partial^2\psi}{\partial z^2} = 0 \quad (1)$$

Let us start with:

$$\nabla^*\nabla\psi_0 = 0 \quad (2)$$

Equation (2) has three-dimensional spherical shape keeping fronts as its solutions. ψ_0 is a scalar function. By changing to polar coordinates it can be deduced that a solution is given by:

$$\psi_0(r,\tau) = \frac{f_0(\boldsymbol{i}r - c\tau)}{r} \quad (3)$$

Where $c = \pm 1$ and $\boldsymbol{i}$ represents a base vector in radial direction. In fact the parameter $\boldsymbol{i}r - c\tau$ of f_0 can be considered as a complex number valued function. It keeps its shape during its travel through the field. Its amplitude quickly diminishes as $1/r$ with distance r from the trigger point.

Next we investigate:

$$\nabla^*\nabla\boldsymbol{\psi} = 0 \quad (4$$

Here $\boldsymbol{\psi}$ is a vector function.

Equation (4) has one-dimensional shape keeping fronts as its solutions:

$$\boldsymbol{\psi}(z,\tau) = \boldsymbol{f}(\boldsymbol{i}z - c\tau) \quad (5)$$

Again the parameter $\boldsymbol{i}z - c\tau$ of $\boldsymbol{f}$ can be interpreted as a complex number based function.

The imaginary $\boldsymbol{i}$ represents the base vector in the x, y plane. Its orientation θ may be a function of z.

That orientation determines the polarization of the one-dimensional shape keeping front.

10.6 Special formulas

$$\boldsymbol{\nabla}\langle\boldsymbol{k},\boldsymbol{x}\rangle = \boldsymbol{k} \quad (1)$$

$\boldsymbol{k}$ is constant.

$$\langle \boldsymbol{\nabla}, \mathbf{x} \rangle = \mathbf{3} \tag{2}$$

$$\boldsymbol{\nabla} \times \mathbf{x} = \mathbf{0} \tag{3}$$

$$\boldsymbol{\nabla} |\mathbf{x}| = \frac{\mathbf{x}}{|\mathbf{x}|} \tag{4}$$

$$\boldsymbol{\nabla} \frac{1}{|\mathbf{x} - \mathbf{x}'|} = -\frac{\mathbf{x} - \mathbf{x}'}{|\mathbf{x} - \mathbf{x}'|^3} \tag{5}$$

$$\langle \boldsymbol{\nabla}, \frac{\mathbf{x} - \mathbf{x}'}{|\mathbf{x} - \mathbf{x}'|^3} \rangle = \langle \boldsymbol{\nabla}, \boldsymbol{\nabla} \rangle \frac{1}{|\mathbf{x} - \mathbf{x}'|} = \langle \boldsymbol{\nabla}, \boldsymbol{\nabla} \frac{1}{|\mathbf{x} - \mathbf{x}'|} \rangle = 4\pi \, \delta(\mathbf{x} - \mathbf{x}') \tag{6}$$

Similar formulas apply to the quaternionic nabla and parameter values.

$$\nabla x = 1 - 3 \; ; \; \nabla^* x = 1 + 3; \; \nabla x^* = 1 + 3$$

$$\nabla (x^* x) = x$$

$$\nabla |x| = \nabla \sqrt{(x^* x)} = \frac{x}{|x|} \tag{7}$$

$$\nabla \frac{1}{|x - x'|} = -\frac{x - x'}{|x - x'|^3} \tag{8}$$

$$\nabla^* \frac{x - x'}{|x - x'|^3} = \nabla \, \nabla^* \frac{1}{|x - x'|} = \left(\frac{\partial}{\partial \tau} \frac{\partial}{\partial \tau} + \langle \boldsymbol{\nabla}, \boldsymbol{\nabla} \rangle \right) \frac{1}{|x - x'|} \neq 4\pi \, \delta(x - x') \tag{9}$$

Instead:

$$(\nabla_0 \nabla_0 + \langle \boldsymbol{\nabla}, \boldsymbol{\nabla} \rangle) \frac{1}{|x|} = \frac{3\tau^2}{|x|^5} - \frac{1}{|x|^3} + \frac{3\tau^2}{|x|^5} = \frac{6\tau^2 - |x|^2}{|x|^5} = \frac{5\tau^2 - |\boldsymbol{x}|^2}{|x|^5} \tag{10}$$

$$(\nabla_0\nabla_0 - \langle \boldsymbol{\nabla}, \boldsymbol{\nabla} \rangle)\frac{1}{|x|} = -\frac{1}{|x|^3} \tag{11}$$

$$\langle \boldsymbol{\nabla}, \boldsymbol{\nabla} \rangle \frac{1}{|\boldsymbol{x}|} = 4\pi\, \delta(\boldsymbol{x}) \tag{12}$$

Thus, with spherical boundary conditions, $\frac{1}{4\pi\,|x-x'|}$ is suitable as the Green's function for the Poisson equation, but $\frac{1}{4\pi\,|x-x'|}$ does not represent a Green's function for the quaternionic operator $(\nabla_0\nabla_0 + \langle \boldsymbol{\nabla}, \boldsymbol{\nabla} \rangle)$!

For a homogeneous second order partial differential equation a Green's function is not required. Thus, the deficit of a green's function does not forbid the existence of a quaternionic homogeneous second order partial differential equation. Still equation (6) forms the base of the Poisson equation.

10.7 Field equations

We will use two sets of differential equations. Both sets use pure space as part of the parameter space.

- Quaternionic differential equations
  - These equations use progression as a parameter.
- Maxwell based differential equations
  - These equations use quaternionic distance as a parameter.

By introducing new symbols $\mathfrak{E}$ and $\mathfrak{B}$ we will turn the quaternionic differential equations into Maxwell-like quaternionic differential equations. We introduce a simple switch $\alpha = \pm 1$ that will turn one set into the other set.

For quaternionic differential calculus is $\alpha = -1$ and $\nabla_0 = \frac{\partial}{\partial \tau}$.

For Maxwell based differential calculus is $\alpha = +1$ and $\nabla_0 = \frac{\partial}{\partial t}$.

In general the following differential equations hold:

$$\phi = \{\phi_0, \boldsymbol{\phi}\} = \{\nabla_0, \boldsymbol{\nabla}\}\{\varphi_0, \boldsymbol{\varphi}\} \tag{1}$$

$$\phi_0 = -\alpha\nabla_0\, \varphi_0 - \langle \boldsymbol{\nabla}, \boldsymbol{\varphi} \rangle \tag{2}$$

$$\boldsymbol{\phi} = \nabla_0\boldsymbol{\varphi} + \boldsymbol{\nabla}\varphi_0 \pm \boldsymbol{\nabla} \times \boldsymbol{\varphi} \tag{3}$$

Equations (2) and (3) are not genuine Maxwell equations. We introduce them here as extra Maxwell equations. Choice $\alpha = 1$ conforms to the Lorenz gauge.

$$\mathfrak{E} \equiv -\nabla_0 \boldsymbol{\varphi} - \boldsymbol{\nabla}\varphi_0 \tag{4}$$

$$\nabla_0 \mathfrak{E} = -\nabla_0 \nabla_0 \, \boldsymbol{\varphi} - \nabla_0 \boldsymbol{\nabla}\varphi_0 \tag{5}$$

$$\langle \boldsymbol{\nabla}, \mathfrak{E} \rangle = -\nabla_0 \langle \boldsymbol{\nabla}, \boldsymbol{\varphi} \rangle - \langle \boldsymbol{\nabla}, \boldsymbol{\nabla} \rangle \varphi_0 \tag{6}$$

$$\mathfrak{B} \equiv \boldsymbol{\nabla} \times \boldsymbol{\varphi} \tag{7}$$

$$\nabla_0 \mathfrak{B} = -\boldsymbol{\nabla} \times \mathfrak{E} \tag{8}$$

$$\langle \boldsymbol{\nabla}, \mathfrak{B} \rangle = 0 \tag{9}$$

$$\boldsymbol{\nabla} \times \mathfrak{B} = \boldsymbol{\nabla} \langle \boldsymbol{\nabla}, \boldsymbol{\varphi} \rangle - \langle \boldsymbol{\nabla}, \boldsymbol{\nabla} \rangle \boldsymbol{\varphi} \tag{10}$$

Also the following equations are not genuine Maxwell equations.

$$\nabla_0 \phi_0 = -\alpha \nabla_0 \nabla_0 \, \varphi_0 - \nabla_0 \langle \boldsymbol{\nabla}, \boldsymbol{\varphi} \rangle \tag{11}$$

$$\boldsymbol{\nabla} \phi_0 = -\alpha \nabla_0 \, \boldsymbol{\nabla} \varphi_0 - \boldsymbol{\nabla} \langle \boldsymbol{\nabla}, \boldsymbol{\varphi} \rangle = -\alpha \nabla_0 \, \boldsymbol{\nabla} \varphi_0 - \boldsymbol{\nabla} \times \boldsymbol{\nabla} \times \, \boldsymbol{\varphi} - \langle \boldsymbol{\nabla}, \boldsymbol{\nabla} \rangle \, \boldsymbol{\varphi} \tag{12}$$

$$\zeta = \{\zeta_0, \boldsymbol{\zeta}\} = \{\nabla_0, -\boldsymbol{\nabla}\}\{\phi_0, \phi\} \tag{13}$$

$$(-\alpha \, \nabla_0 \nabla_0 + \langle \boldsymbol{\nabla}, \boldsymbol{\nabla} \rangle)\varphi = \zeta_0 + \boldsymbol{\zeta} \tag{13}$$

$$\zeta_0 = (-\alpha \nabla_0 \nabla_0 + \langle \boldsymbol{\nabla}, \boldsymbol{\nabla} \rangle)\varphi_0 = \nabla_0 \, \phi_0 - \langle \boldsymbol{\nabla}, \mathfrak{E} \rangle \tag{14}$$

$$\boldsymbol{\zeta} = (-\alpha \nabla_0 \nabla_0 + \langle \boldsymbol{\nabla}, \boldsymbol{\nabla} \rangle)\boldsymbol{\varphi} = -\boldsymbol{\nabla}\phi_0 + \alpha \nabla_0 \mathfrak{E} - \boldsymbol{\nabla} \times \boldsymbol{\mathcal{B}} \tag{15}$$

$$\rho_0 = \langle \boldsymbol{\nabla}, \boldsymbol{\nabla} \rangle \varphi_0 = \zeta_0 + \, \alpha \, \nabla_0 \nabla_0 \varphi_0 \tag{16}$$

$$\boldsymbol{\rho} = \langle \boldsymbol{\nabla}, \boldsymbol{\nabla} \rangle \boldsymbol{\varphi} = \boldsymbol{\zeta} + \alpha \, \nabla_0 \nabla_0 \boldsymbol{\varphi} \tag{17}$$

Thus a simple change of a parameter and the control switch α turn quaternionic differential equations into equivalent Maxwell based differential equations and vice versa. This makes clear that both sets represent two different views from the same subject, which is a field that can be stored in the eigenspace of an operator that resides in the Gelfand triple.

10.8 Solutions of the wave equation

The Maxwell based differential calculus offers second order partial differential equations in the form of the wave equations:

$$(\nabla_0\nabla_0 - \langle \boldsymbol{\nabla}, \boldsymbol{\nabla} \rangle)\varphi_0 = \frac{\partial^2\varphi_0}{\partial\tau^2} - \frac{\partial^2\varphi_0}{\partial x^2} - \frac{\partial^2\varphi_0}{\partial y^2} - \frac{\partial^2\varphi_0}{\partial z^2} = \rho_0 \tag{1}$$

$$(\nabla_0\nabla_0 - \langle \boldsymbol{\nabla}, \boldsymbol{\nabla} \rangle)\boldsymbol{\varphi} = \frac{\partial^2\boldsymbol{\varphi}}{\partial\tau^2} - \frac{\partial^2\boldsymbol{\varphi}}{\partial x^2} - \frac{\partial^2\boldsymbol{\varphi}}{\partial y^2} - \frac{\partial^2\boldsymbol{\varphi}}{\partial z^2} = \boldsymbol{\rho} \tag{2}$$

10.8.1 Shape keeping fronts

Like the quaternionic second order partial differential equation this wave equation offers solutions that represent shape keeping fronts.

For isotropic conditions in three participating dimensions the shape keeping front solution runs:

$$\varphi_0 = f(r - ct)/r, \text{ where } c = \pm 1; f \text{ is real} \tag{3}$$

This follows from

$$\langle \nabla, \nabla \rangle \varphi_0 \equiv \frac{1}{r^2}\left(\frac{\partial}{\partial r}\left(r^2\frac{\partial\varphi_0}{\partial r}\right)\right) = \frac{f''(r - ct)}{r} = \frac{1}{c^2}\frac{\partial^2\varphi_0}{\partial t^2} \tag{4}$$

In a single participating dimension the shape keeping front solution runs:

$$\varphi_0 = f(x - ct), \text{ where } c = \pm 1; f \text{ is real} \tag{5}$$

The same solutions hold for vector function $\boldsymbol{\varphi}$.

10.8.2 Other solutions of the homogenous wave equation

Apart from the shape keeping solutions the homogeneous wave equation offers wave form solutions. Some of these solutions are obtained by starting with:

$$\nabla_0\nabla_0 f = \langle \boldsymbol{\nabla}, \boldsymbol{\nabla} \rangle f = -\omega^2 f \tag{1}$$

$$f(t, \boldsymbol{x}) = a\exp\big(i\omega(ct - |\boldsymbol{x} - \boldsymbol{x}'|)\big)\,; c = \pm 1 \tag{2}$$

This leads to a category of solutions that are known as solutions of the Helmholtz equation.

10.8.3 The Maxwell based Poisson equations

The screened Poisson equation in Maxwell based differential calculus runs:

$$(\langle \boldsymbol{\nabla}, \boldsymbol{\nabla} \rangle - \lambda^2)\varphi = \frac{\partial^2 \varphi}{\partial x^2} - \frac{\partial^2 \varphi}{\partial y^2} - \frac{\partial^2 \varphi}{\partial z^2} - \lambda\varphi = -\rho \tag{1}$$

$$\frac{\partial^2 \varphi}{\partial t^2} = \lambda^2 \varphi \tag{2}$$

$$\varphi = a(\boldsymbol{x})\exp(\pm\lambda t) \tag{3}$$

This differs significantly from the quaternion differential calculus version of the screened Poisson equation.

10.9 Asymmetric tensor

The Maxwell-based equation

$$\phi \Leftrightarrow \{\phi_0, \boldsymbol{\phi}\} \Leftrightarrow \{\nabla_0, \boldsymbol{\nabla}\}\{\varphi_0, \boldsymbol{\varphi}\} = \{\nabla_0, -\boldsymbol{\nabla}\}\{A_0, \boldsymbol{A}\} \tag{1}$$

$$\boldsymbol{\phi} = -\mathfrak{E} \pm \mathfrak{B} \tag{2}$$

$$\mathfrak{E}_\nu \equiv -\left(\frac{\partial \varphi_0}{\partial x_\nu} + \frac{\partial \varphi_\nu}{\partial t}\right) = -F_{0\nu} = \partial_0 A_\nu - \partial_\nu A_0; \nu = 1..3 \tag{3}$$

$$\mathfrak{B}_{\mu\nu} = (\boldsymbol{\nabla} \times \boldsymbol{\varphi})_{\mu\nu} = \left(\frac{\partial \varphi_\mu}{\partial x_\nu} - \frac{\partial \varphi_\nu}{\partial x_\mu}\right) = \partial_\mu A_\nu - \partial_\nu A_\mu; \mu = 1..3; \nu = 1..3; \tag{4}$$

corresponds with the asymmetric tensor $F_{\mu\nu}$

$$F_{\mu\nu} = \partial_\mu A_\nu - \partial_\nu A_\mu = \begin{bmatrix} 0 & -\mathfrak{E}_x & -\mathfrak{E}_y & -\mathfrak{E}_z \\ \mathfrak{E}_x & 0 & \mp\mathfrak{B}_z & \pm\mathfrak{B}_y \\ \mathfrak{E}_y & \mp\mathfrak{B}_z & 0 & \mp\mathfrak{B}_x \\ \mathfrak{E}_y & \pm\mathfrak{B}_y & \mp\mathfrak{B}_x & 0 \end{bmatrix} \tag{5}$$

For the quaternionic differential calculus the ***same tensor*** can be generated. The tensor does not show the nature of the partial derivatives that are contained in the $\mathfrak{E}_\nu$ terms. The tensor hides the real parts of the differential.

This means that equation

$$\phi_0 = -\alpha\nabla_0\,\varphi_0 - \langle \boldsymbol{\nabla}, \boldsymbol{\varphi} \rangle \tag{6}$$

is ignored. This equation contains the sign switch α.

10.1 The space-progression model

This paper supports two space progression models. Quaternions, quaternionic functions and quaternionic differential equations support parameter spaces that have an Euclidean signature and correspond to a metric tensor:

$$g_{\mu\nu} = \begin{bmatrix} 1 & 0 & 0 & 0 \\ 0 & 1 & 0 & 0 \\ 0 & 0 & 1 & 0 \\ 0 & 0 & 0 & 1 \end{bmatrix} \tag{1}$$

Elements of this model can directly be stored as eigenvalues in quaternionic Hilbert spaces.

The Maxwell based equations and the parameter space of these equations support a space-time model with Minkowski signature and correspond to a metric tensor:

$$g_{\mu\nu} = \begin{bmatrix} 1 & 0 & 0 & 0 \\ 0 & -1 & 0 & 0 \\ 0 & 0 & -1 & 0 \\ 0 & 0 & 0 & -1 \end{bmatrix} \tag{2}$$

Elements of this model must first be dismantled into their real components before they can be stored as eigenvalues in Hilbert spaces.

The fact that the quaternionic field can be stored in the eigenspace of an operator that resides in a non-separable quaternionic Hilbert space and that after dismantling into real components the same can be done for a Maxwell based field means that the stored fields can represent one and the same object. It also means that both differential equation sets can investigate the same field and offer different views onto that field that reveal different aspects of the behavior of that field.

It also means that both space-progression models represent different views of the same reality.

11 Embedding

11.1 Selection

At each progression instant only a single eigenvalue a_i^x is selected from the eigenspace of the symmetry center reference operator $\mathfrak{S}_n^x$. In a regeneration cycle a complete location swarm $\{a_i^x\}$ of eigenvalues is selected. The set $\{a_i^x\}$ correspond to sets of eigenvectors $\{|a_i^x\rangle\}$ that span a corresponding subspace. This restricts reference operator $\mathfrak{S}^x = |\mathfrak{s}_i^x\rangle\mathfrak{s}_i^x\langle\mathfrak{s}_i^x|$ to operator $\sigma^x = |a_j^x\rangle a_j^x\langle a_j^x|$. The corresponding closed subspace acts as a sliding window within a larger subspace that covers all progression values, including the history of the sliding window. The sliding window covers the recurrent regeneration of the set $\{a_i^x\}$. During this period the statistical properties of the set stabilize. The set $\{a_i^x\}$ inherits the symmetry flavor of the symmetry center. Its elements are selected in a stochastic fashion that is independent of the spatial ordering of the symmetry center.

11.2 Suggested generation process

The mechanism $\mathfrak{M}_n$,which controls the generation of the set of eigenvalues $\{a_i^x\}$ of stochastic operator σ^x, might apply a Poisson process in combination with a binomial process. The mechanism

works in sync with the progression steps that are defined by reference operator $\mathcal{R}^{⓪}$. At regular instances, the Poisson process produces germs that are spread by the binomial process, which implements a spread function that converts the germs into the ***spatial location swarm*** $\{a_i^x\}$. The spread function produces locations that are selected from the symmetry center $\mathfrak{S}_n^x$. The binomial process effectively attenuates the spatial effectivity of the Poisson process. A Poisson process in combination with a binomial process can be considered as a new Poisson process. This time the stochastic process is spatially distributed. We shall refer to this special stochastic process as a ***stochastic spatial spread function*** $\mathcal{S}_n(\mathfrak{s}_i^x)$ that blurs the location of the geometric center of the swarm. This geometric center coincides with the geometric center of the symmetry center.

The spread function is spherical symmetric and is best treated in spherical coordinates. The generated location is specified in the independent variables radius r, polar angle φ and azimuth θ. The order of these specifications may vary between mechanism types. This order and the direction in which the angles run influence the generated ***hopping path***.

This view makes it possible to treat the swarm as a point spread function that can be handled in a similar way as the point spread function in an imaging process. This means that optical Fourier methodology can be used in order to handle the movement and mappings of the swarm. For that purpose it is necessary that the point spread function owns a Fourier transform. We will apply that Fourier transform as a coherence quality characteristic of the generated swarm. The swarm is mapped onto the embedding continuum. This map will be considered as the imaging process. The map will treated as an Optical Transfer Function. This means that the Fourier transform of the mapped swarm equals product of the Fourier transform of the generated swarm and the Optical Transfer Function of the map.

For a swarm, owning a Fourier transfer means owning a displacement generator. It means that in first approximation the swarm can be considered as moving as one unit.

After finishing the generation cycle the stochastic spatial spread function can be considered as a ***location density distribution***.

11.3 Regeneration and detection

The regeneration of an elementary particle by the controlling mechanism $\mathfrak{M}_n$ involves the creation of a new embedding location. Detection stops this regeneration process. At detection, the set $\{a_i^x\}$ is no longer filled by taking locations from the members of the set $\{\mathfrak{s}_i^x\}$. No more elements of the set are stored in the separable Hilbert space. With other words, afterwards detection occurred at a precisely known location. However, that location was not known beforehand.

A virtual map images the completely regenerated set $\{a_i^x\}$ onto parameter space $\mathcal{R}^{⓪}$. This involves the reordering from the stochastic generation order to the ordering of this new parameter space. This first map turns the location swarm into the eigenspace of a virtual operator $\mathscr{b}$. A continuous location density distribution $\xi(q)$ describes the virtual map of the swarm into parameter space $\mathfrak{R}^{⓪}$. Actually each element of the original swarm is embedded into the deformable embedding continuum $\mathfrak{C}$ where that element is blurred with the Green's function of this embedding continuum.

This indirectly converts the operator $\mathscr{o}$, which describes the regeneration in the symmetry center $\mathfrak{S}_n^x$ into a differently ordered operator ξ that resides in the Gelfand triple $\mathcal{H}$. The defining function $\xi(q)$ of operator ξ describes the triggers in the non-homogeneous quaternionic second order partial differential equation, which describes the embedding behavior of $\mathfrak{C}$.

(1)

$$\xi = \nabla^*\nabla\psi = \{\nabla_0\nabla_0 + \langle \boldsymbol{\nabla}, \boldsymbol{\nabla}\rangle\}\psi = \frac{\partial^2\psi}{\partial\tau^2} + \frac{\partial^2\psi}{\partial x^2} + \frac{\partial^2\psi}{\partial y^2} + \frac{\partial^2\psi}{\partial z^2}$$

Function $\xi(q)$ uses $\mathfrak{R}^{⓪}$ as its parameter space. $\mathscr{o}$ describes the hopping of the point-like object, while $\xi(q)$ describes the density distribution of the corresponding location swarm.

Stochastic operator $\mathscr{o}$ describes the hopping of the point-like object, while ξ describes the density distribution of the image of the corresponding location swarm.

Most of the described map is virtual. Only the embedding or the detection are actual occurrences. The consequences of detection and the consequences of the embedding can be observed.

11.4 The mapper

The mapper function $\wp^x(q)$ maps elements a_i^x of location swarms $\{a_i^x\}$ onto the continuum $\mathfrak{C}$, which is defined by function $\mathfrak{C}(q)$. The mapper $\wp^x = \wp^x(\mathbf{0})$ maps the geometric center of the symmetry center onto a location in the continuum $\mathfrak{C}$.

The action of the mapper function can be split into four steps. The intermediate steps are virtual maps. We introduce these virtual steps in order to be able to analyze what happens.

The three first steps form a map from a subset of the eigenspace of $\mathfrak{S}_n^x$ to the corresponding eigenspace of $\mathfrak{R}^{⓪}$.

The first step stores selections into the eigenspace of ***stochastic selection operator*** $\mathscr{o}^x$. The operator $\mathscr{o}^x = |a_j^x\rangle a_j^x \langle a_j^x|$ resides in separable Hilbert space $\mathfrak{H}$ and represents the discrete location distribution $\{a_j^x\}$ that is generated by the stochastic spatial spread function $\mathcal{S}_n(\mathfrak{s}_i^x)$ during a period of progression that covers the progression values of the set $\{a_j^x\}$.Afterwards, $\mathcal{S}_n(\mathfrak{s}_i^x)$ acts as a location density distribution. Operator $\mathscr{o}^x$ is a stochastic operator.

The second step maps $\{a_j^x\}$. onto $\boldsymbol{\mathcal{R}}^{⓪}$.

$$b_j^x = \mathscr{g}(a_j^x, n) \qquad (1)$$

The second step maps the geometric center of the symmetry center onto location $\mathscr{g}(\mathbf{0}, n)$ in $\boldsymbol{\mathcal{R}}^{⓪}$. The second step switches the symmetry flavor of the swarm $\{\boldsymbol{a}_j^x\}$ into $\{\boldsymbol{b}_j^{⓪}\}$ and then maps onto $\boldsymbol{\mathcal{R}}^{⓪}$. $b_j^{⓪}$ keeps the real value of a_j^x. This involves relocation of the set of eigenvalues. The ***mapped selection operator*** $\mathscr{b}^{⓪} = |b_j^{⓪}\rangle\, b_j^{⓪}\, \langle b_j^{⓪}|$, resides in separable Hilbert space $\mathfrak{H}$ and represents the discrete distribution $\{b_j^x\}$ that is indirectly generated by the stochastic spatial spread function $\mathcal{S}_n(\mathfrak{s}_i^x)$ during a period of progression that covers the progression values of the set $\{a_j^x\}$. This set is the map onto parameter space $\mathcal{R}^{⓪}$ and it is relocated due to the displacement of the symmetry center by field $\mathfrak{A}$. Operator $\mathscr{b}^{⓪}$ is in effect also a stochastic operator. The real parts of operators $\mathscr{o}^x$ and $\mathscr{b}^{⓪}$ were already synchronized with each other and are in sync (but not in sequence order) with the progression values that are specified by the Hermitian part $\mathcal{R}_0^{⓪}$ of the reference operator $\mathcal{R}^{⓪}$.

The mapper $\wp^x$ is affected by the movements of the symmetry related charges that are initiated by the symmetry related field $\mathfrak{A}$. It means that the symmetry centers on which the coherent location swarms reside are ***relocated*** due to the effects of the symmetry related field $\mathfrak{A}$ on the

locations of the symmetry related charges. This influences function $\mathscr{g}$ in equation (1). The symmetry related charges are located at the geometric centers of the symmetry centers. They are point-like objects and are located at $\mathscr{g}(\mathbf{0}, n)$. The symmetry related field is constituted from the contributions that are generated by the individual symmetry related charges. The symmetry related field $\mathfrak{A}$ uses $\mathfrak{R}^{⓪}$ as its parameter space. As a consequence the

The displacement can be interpreted as a usually uniform movement of the symmetry center. This results in a distorted image $\left\{b_j^{⓪}\right\}$ of swarm $\{a_j^x\}$ on parameter space $\mathcal{R}^{⓪}$. The swarm is no longer characterized by the stochastic spatial spread function $\mathcal{S}_n(\mathfrak{s}_i^x)$. If the displacement is small compared to the extension of the swarm, then the distorted swarm can still be characterized by a continuous location density distribution. That new location density distribution is not obtained via normal distortion of the complete original location density distribution. Instead every separate element is displaced in an individual way that is determined by its progression order. The new shape cannot be predicted from the old shape. We will attach a new name $\xi_n(\boldsymbol{q})$ to this location density distribution. It replaces the stochastic spatial spread function $\mathcal{S}_n(\mathfrak{s}_i^x)$.

This sidetrack has no influence on the mapper $\wp^x$. Mapper $\wp^x$ treats the relocation of the geometric center $\mathscr{g}(\mathbf{0}, n)$ of the symmetry center $\mathfrak{S}_n^x$. However, the redistribution influences mapper function $\wp^x(q)$.

The third step embeds $\mathfrak{H}$ into $\mathcal{H}$ by mapping $\mathcal{R}^{⓪}$ onto $\mathfrak{R}^{⓪}$. It is a map between quaternions with rational valued components and a continuum consisting of quaternions that have real valued components. The discrete set and the continuum have the same symmetry flavor, which is the reference symmetry flavor. The geometric center $\mathscr{g}(\mathbf{0}, n)$ of the symmetry center $\mathfrak{S}_n^x$ has a similar value in $\mathfrak{R}^{⓪}$.

In this step operator $\mathscr{b}^{⓪}$ gets accompanied by operator ξ, which represents the continuous density distribution that characterizes the eigenspace $\left\{b_j^{⓪}\right\}$ of $\mathscr{b}^{⓪}$. Generating the eigenspace of operator ξ in the separable Hilbert space involves a local averaging over the full regeneration cycle and resampling of the generated $b_j^{⓪}$ locations. This offers a density distribution that is characterized by $\xi(q_i)$. Operator ξ plays no significant role in the embedding process. ***Its role is purely administrative***. It relates $\left\{b_j^{⓪}\right\}$ to the wave function of the elementary object. Further, it enables the computation of the embedding field potential, which is a smoothed and averaged view of the embedding continuum. If $\xi(q_i)$ has a Fourier transform, then the existence of $\xi(q_i)$ is the assurance of the coherence of the location swarm. It means that the mapped swarm has a displacement generator and at first approximation it can be considered to move as one unit.

The fourth step is performed completely inside $\mathcal{H}$ by operator $\mathfrak{C}$. This involves the blurring of the elements of $\left\{b_j^{⓪}\right\}$ by the Green's function $\mathcal{G}$ of the embedding continuum.

In the four steps, operator $\mathscr{o}$ is transferred to operator $\mathscr{b}$, reordered, relocated and smoothed, such that operator ξ results. The embedding process then blurs the swarm further. The result is a rather smooth, but deformed embedding field $\mathfrak{C}$. For a part, the embedding process can be described by second order partial differential equations.

The described multi-step map from generation to embedding is in fact a virtual map that occurs in one instant. Its structure is only of interest when the generation of the swarm suddenly stops. The smoothing effect of the Green's function $\mathcal{G}(q)$ of the embedding process and the integration over the generation cycle normally hide the structure of the route that is taken.

The symmetry flavor switch occurs in $\mathfrak{H}$ and the deformation of the continuum by the embedding process occurs in $\mathcal{H}$.

Apart from the conversion of the symmetry flavor and the relocation $\mathcal{g}(q,n)$ of the symmetry center the mapper $\wp^x$equals the map onto the embedding continuum.

Thus for the mapper function $\wp^x(q)$ holds:

$$\wp^x(q) = \mathfrak{C}(\mathcal{g}(q,n)) \circ \mathcal{G}(q) \tag{1}$$

And for the mapper $\wp^x$ holds:

$$\wp^x = \wp^x(\mathbf{0}) = \mathfrak{C}(\mathcal{g}(\mathbf{0},n)) \tag{2}$$

This location is not embedded, thus is not blurred by a Green's function.

If we include the blur that is introduced by the generation process, then the total map can be characterized by:

$$\mathcal{P}(q) = \wp^x \circ \xi_n = \ \mathfrak{C}\big(\mathcal{g}(q,n)\big) \circ \mathcal{G}(q) \circ \xi_n(q) = \mathfrak{C}\big(\mathcal{g}(q,n)\big) \circ \mathfrak{G}(q) \tag{3}$$

$\xi_n(q)$ is the location density distribution that replaces the stochastic spatial spread function $\mathcal{S}_n(\mathfrak{s}_i^x)$. The stochastic spatial spread function varies with each subsequent generation cycle. The location density distribution $\xi_n(q)$ depends on the movement of the symmetry center $\mathfrak{S}_n^x$. Fourier transformation converts convolution into multiplication.

$$\widetilde{\mathfrak{G}}(\tilde{q}) = \tilde{\mathcal{G}}(\tilde{q}) \circ \tilde{\xi}_n(\tilde{q}) \tag{4}$$

$\widetilde{\mathfrak{G}}(\tilde{q})$ ***qualifies the coherence of the map***.

The exact target location $\mathcal{P}\big(a_j^x\big)$ is not known beforehand, but after selection of the source eigenvalue a_j^x the image $\wp^x\big(a_j^x\big)$ is exactly known and is stored in the eigenspaces of the respective operators. With other words history is no longer uncertain and is accurately stored in the separable Hilbert space and in its companion Gelfand triple.

Averaged over all selections, $\mathcal{P}$ produces a blurred image of the set $\{a_j^x\}$. The blur is characterized by $\mathfrak{G}(q)$. The blur only concerns the imaginary parts of the involved quaternions.

The average $\boldsymbol{a}^x$ of the imaginary parts of all $\{a_j^x\}$ is the center location of the set. It corresponds to the geometric center of the symmetry center. The combination of all involved operators and the selection mechanism $\mathfrak{M}_n$ produces a blurred image of $\boldsymbol{a}^x$.

11.5 Coherence

Closed subspaces of a separable Hilbert space are characterized by a countable set of eigenvalues of a normal operator that maps this subspace onto itself.

The eigenvalues of the operators in quaternionic Hilbert spaces are quaternions. Due to the four dimensions of quaternions, quaternionic number systems exist in 16 versions that only differ in their discrete symmetry set. For example right handed quaternions exist and left handed quaternions exist.

Dedicated mechanisms $\{\mathfrak{M}_n\}$ ensure the coherence of the set of selected eigenvalues. For each coherent set $\{a_i^x\}$ the responsible mechanism $\mathfrak{M}_n$ takes the eigenvalues from the eigenspace of a symmetry center reference operator $\mathfrak{S}_n^x$ and stores them in the eigenspace of the stochastic operator σ^x. The swarm $\{a_i^x\}$ is characterized by a location density distribution $\mathcal{S}_n(\mathfrak{s}_i^x)$.

In the model, coherence plays an important role. For that reason the mapping of the swarm $\{a_j^x\}$ of eigenvalues of stochastic operator σ^x onto the embedding continuum $\mathfrak{C}$ is analyzed in detail in order to ensure that coherence is not destroyed by the mapping process.

The following criteria define the set $\{a_i^x\}$ of selected discrete quaternionic eigenvalues as a ***coherent set***:

1. All members of the set $\{a_i^x\}$ are taken from the same symmetry center.
    a. All members of the set belong to the same symmetry flavor.
    b. All members of the set have the same spin value.
    c. The selected set is well-ordered.
2. The set can be described by a continuous density distribution.

An ***ordered coherent set*** is ordered with respect to the real parts of its members. In a ***well-ordered coherent set*** all members have different real parts.

The second requirement means that the spread function $\mathcal{S}_n$ can be considered as a continuous location density distribution.

The well-ordered coherent set $\{a_i^x\}$ describes a well-defined hopping path. Also the hops form a discrete distribution. The distribution of the hops is described by operator $\boldsymbol{\sigma}^x$, which is the anti-Hermitian part of operator σ^x. The landing locations form a well ordered swarm and the hops are also ordered with respect to progression. However, the subsequent hops have quite stochastic directions and sizes. Like the Hermitian part, the anti-Hermitian part of σ^x has no continuous defining function! The location density distribution $\mathcal{S}_n(\mathfrak{s}_i^x)$ that describes the set of locations also characterizes the distribution of the hop landing locations.

The real valued continuous location density distribution $\xi_0(q^{⓪})$ describes the density distribution of set $\{b_j^x\}$ with respect to parameter space $\mathcal{R}^{⓪}$. In fact this density distribution is the real part of the defining function of operator ξ. However, in the eigenspace of ξ_0 the spatial eigenvalues are reordered, relocated and smoothed when compared to the eigenvalues $\{a_i^x\}$ of the stochastic operator σ^x.

Function $\xi(q^{⓪})$ describes the defining function of operator ξ. The only purpose of this operator is to show the coherence of the generated and relocated swarm $\{b_j^x\}$. Function $\xi(q^{⓪})$ has a

Fourier transform. This Fourier transform is used to qualify the coherence of the relocated swarm $\{b_j^x\}$. That is why we add as extra requirement for the coherence of swarm $\{b_j^x\}$ that it owns a Fourier transform. Having a Fourier transform is a higher level coherence requirement.

We will qualify a location swarm $\{\boldsymbol{b}_j^x\}$ that owns a Fourier transform as a ***coherent swarm***.

11.1 Coherent swarm

The well-ordered coherent set $\{\boldsymbol{b}_j^x\}$, which can be described by a dynamic continuous location density distribution $\xi_0(q^x)$ may via this relation also own a Fourier transform. In that case we call the set a ***coherent swarm***. The coherent swarm owns a displacement generator. This means that at first approximation the swarm $\{\boldsymbol{b}_j^x\}$ ***moves as one unit***. Owning a Fourier transform is a higher level coherence requirement.

At uniform speed $\boldsymbol{v}$ holds:

$$\boldsymbol{\xi}(q^{⓪}) = \boldsymbol{v}\,\xi_0(q^{⓪}) \tag{1}$$

Owning a Fourier transform via a continuous location density distribution means that the swarm can be represented by a wave package. On movement, wave packages tend to disperse. Since the dynamic continuous location density distribution only describes the swarm, the density distribution is continuously regenerated. As a consequence, movement does not disperse the swarm's wave package. Thus, due to recurrent regeneration, no danger of dispersion exists.

On the other hand the representation by a wave package indicates that the swarm $\{b_j^x\}$ may take the form of an interference pattern. That interference pattern is still a location swarm. It is not constructed by interfering waves!

11.2 Embedding set elements

Embedding a single element a_j^x of the subset $\{a_j^x\}$ of the eigenspace of σ^x in continuum $\mathfrak{C}$ involves first the conversion to the reference symmetry flavor. Next this element is mapped from the symmetry center to the eigenspace of $\mathcal{R}^{⓪}$ in $\mathfrak{H}$ and subsequently into to the eigenspace of $\mathfrak{R}^{⓪}$ in $\mathcal{H}$. The symmetry related fields may have caused a relocation of the symmetry center with respect to $\mathcal{R}^{⓪}$. Finally the discrete quaternion is embedded as a discrete artefact in continuum $\mathfrak{C}$.

Locally the curved continuum $\mathfrak{C}$ is represented by ψ, which usually is nearly flat. In that case, for ψ we can use the quaternionic nabla ∇.

$$\nabla = \nabla_0 + \boldsymbol{\nabla} = \left\{\frac{\partial}{\partial\tau}, \frac{\partial}{\partial x}, \frac{\partial}{\partial y}, \frac{\partial}{\partial z}\right\};\ \psi = \psi_0 + \boldsymbol{\psi} \tag{1}$$

As alternative we can use the Maxwell based differential calculus. This calculus uses:

$$\{\nabla_t, \boldsymbol{\nabla}\} \Leftrightarrow \left\{\frac{\partial}{\partial t}; \frac{\partial}{\partial x}, \frac{\partial}{\partial y}, \frac{\partial}{\partial z}\right\};\ \psi \Leftrightarrow \{\psi_0, \boldsymbol{\psi}\}; t \Leftrightarrow |\tau + \boldsymbol{x}| \tag{2}$$

ψ is considered to cover the image of the local symmetry center. Thus, it covers the images of all elements of $\{a_j^x\}$. This makes ψ a normalizable function.

The duration of the embedding is very short and is quickly released. Current mathematics lacks a proper description of the full embedding process, but it already contains equations that properly describe the situation before, after and during the embedding.

What happens under not too violent conditions and over not too long ranges can be described by the non-homogeneous second order partial differential equations.

$$\nabla\nabla^{*}\psi = (\nabla_0\nabla_0 + \langle\boldsymbol{\nabla},\boldsymbol{\nabla}\rangle)\psi = \xi \tag{3}$$

$$\left(\frac{\partial}{\partial t}\frac{\partial}{\partial t} - \langle\boldsymbol{\nabla},\boldsymbol{\nabla}\rangle\right)\psi_0 = \rho_0 \tag{4}$$

$$\left(\frac{\partial}{\partial t}\frac{\partial}{\partial t} - \langle\boldsymbol{\nabla},\boldsymbol{\nabla}\rangle\right)\boldsymbol{\psi} = \boldsymbol{\rho} \tag{5}$$

For a single embedding event the right side of these equations take the form of a Dirac delta function.

Directly before and after the embedding the right parts of the equations are equal to zero. In this condition any solution of the homogeneous second order partial differential equation will proceed as it did before.

During the embedding the right parts of the equations represent the embedded discrete quaternion, which is treated as an artifact that can cause a local point-like discontinuity. The embedding results in the emission of a spherical shape keeping front, which is a solution of the homogeneous second order partial differential equation. The non-homogeneous second order partial differential equation may be limited by special conditions:

$$\nabla_0\nabla_0\psi = -\lambda^2\,\psi;\ \psi = a(\boldsymbol{x})\exp(\pm i\,\omega\,\tau) \tag{6}$$

$$\frac{\partial}{\partial t}\frac{\partial}{\partial t}\psi_0 = -\lambda^2\,\psi_0;\ \psi_0 = a_0(\boldsymbol{x})\exp(\pm\,\lambda\,t) \tag{7}$$

$$\frac{\partial}{\partial t}\frac{\partial}{\partial t}\boldsymbol{\psi} = -\lambda^2\,\boldsymbol{\psi};\ \boldsymbol{\psi} = \boldsymbol{a}(\boldsymbol{x})\exp(\pm\,\lambda\,t) \tag{8}$$

This reduces the quaternionic non-homogeneous second order partial differential equation to a screened Poisson equation:

$$\langle\boldsymbol{\nabla},\boldsymbol{\nabla}\rangle\psi - \lambda^2\psi = \xi \tag{9}$$

The 3D solution of this equation is determined by the screened Green's function $G(r)$.

Green functions represent solutions for point sources.

$$G(r) = \frac{\exp(-\lambda\, r)}{r} \tag{10}$$

$$\psi = \iiint G(\boldsymbol{r} - \boldsymbol{r}')\, \rho(\boldsymbol{r}')\, d^3\boldsymbol{r}\,' \tag{11}$$

The Maxwell based differential calculus gives similar results as quaternionic differential calculus does. However, equations (7) and (8) differ significantly from equation (6). The frequency in equation (6) can be used to synchronize the embedding process with the progression step that is governing reference operator $\mathcal{R}^{⓪}$.

The continuum is touched and as a reaction it gets deformed. The embedded particle location will vanish, but traces in the continuum stay and represent the deformation. However, also these traces fade away. Only the recurrence of the generation and embedding processes keeps the deformation fairly steady.

Solutions of the quaternionic second order partial differential equation can be found via the continuity equations:

$$\nabla\psi = \phi\ ;\ \nabla^*\phi = \xi \tag{12}$$

And

$$\nabla^*\psi = \zeta\ ;\nabla\,\zeta = \xi \tag{13}$$

11.2.1 Solutions of the homogeneous equation

Solutions of the homogeneous second order partial differential equation that cover an odd number of dimensions are known to represent shape keeping fronts or combinations of shape keeping fronts. These shape keeping fronts proceed with fixed speed c. However, due to their diminishing amplitude, the spherical shape keeping fronts fade away.

In addition to this the Maxwell based wave equation offers solutions that represent dynamic waves and dynamic oscillations.

Embedding a single element of $\{a_j^x\}$ may cause the emission of a single spherical shape keeping front. The amplitude of spherical shape keeping fronts diminishes as 1/r with distance r from the source. This is also the form of the Green's function of the Poisson equation for the three dimensional isotropic case. This fact forms the origin of the deformation of the embedding continuum ψ.

Embedding a single hop may cause the emission of a single one-dimensional shape keeping front. The amplitude of one-dimensional shape keeping fronts keeps constant. The direction of the one dimensional shape keeping front relates to the direction of the hop. This phenomenon may represent quanta that leave or enter the object that is represented by the swarm $\{a_j^x\}$.

11.2.2 Embedding hops

The content of this section is speculative.

A hop involves de-embedding, a space step $\psi_A \longrightarrow \psi_B$ and re-embedding. This suggests the combined action of two coupling equations:

$$\nabla\psi_A = m_1\,\xi^* \tag{1}$$

and

$$\nabla^*\xi^* = m_2\psi_B \tag{2}$$

Notice that

$$(\nabla\xi)^* = \nabla_0\xi_0 - \nabla_0\boldsymbol{\xi} - \boldsymbol{\nabla}\xi_0 - \langle\boldsymbol{\nabla},\boldsymbol{\xi}\rangle - \boldsymbol{\nabla}\times\boldsymbol{\xi}$$

$$\nabla^*\xi^* = \nabla_0\xi_0 - \nabla_0\boldsymbol{\xi} - \boldsymbol{\nabla}\xi_0 - \langle\boldsymbol{\nabla},\boldsymbol{\xi}\rangle + \boldsymbol{\nabla}\times\boldsymbol{\xi}$$

This produces the equation:

$$\nabla^*\nabla\psi_A = \frac{\partial^2\psi_A}{\partial\tau^2} + \frac{\partial^2\psi_A}{\partial x^2} + \frac{\partial^2\psi_A}{\partial y^2} + \frac{\partial^2\psi_A}{\partial z^2} = m_1 m_2\psi_B \tag{3}$$

With $m_1 m_2 \to m^2$ and $\psi_A \approx \psi_B \to \psi$ this resembles the quaternionic form of the Klein-Gordon equation:

$$\frac{\partial^2\psi}{\partial\tau^2} + \frac{\partial^2\psi}{\partial x^2} + \frac{\partial^2\psi}{\partial y^2} + \frac{\partial^2\psi}{\partial z^2} = m^2\,\psi \tag{4}$$

For curl free conditions and $\xi = \psi$, the coupling equations (1) and (2) resemble the Dirac equations [12]. This suggests that other elementary particles than electrons and positrons follow equations that are similar to equations (1) and (2), where equation (2) treats the antiparticle.

$$\xi = m^2\,\psi \tag{5}$$

It is striking that in equation (4) m appears as squared, while in the continuity equations m appears as a linear factor. The model suggests that the contributions of the swarm elements just add and that m should be proportional to the number of swarm elements.

11.3 Embedding the full set

If the full set is considered, then this means that the view integrates over the full cycle of progression steps that represent the generation of the swarm $\{a_j^x\}$.

If embedding of the full set $\{a_j^x\}$ is considered, then ξ represents the density distribution of the full set. In that case the continuity equations: $\nabla\,\zeta = \rho$ and $\nabla^*\phi = \xi$ determine what happens to the embedding continuum ψ, which locally represents $\mathfrak{C}$. As already indicated, due to the relocation of the source region and the deformation the map of ξ may flow and deform relative to ψ.

The set $\{a_j^x\}$ is well-ordered with respect to progression. It means that each of its elements only exists during a small interval. Before that interval the element did not exist. It is ***generated*** by stochastic process that is controlled by a stochastic mechanism $\mathfrak{M}_n$. The stochastic process applies a stochastic spatial spread function $\mathcal{S}_n(\mathfrak{s}_i^x)$. After the embedding this element of $\{a_j^x\}$ vanishes into history. $\mathcal{S}_n$ can be interpreted as a continuous location density distribution. Only its value is stored in an eigenvalue of operator $\sigma^x = |a_j^x\rangle a_j^x \langle a_j^x|$ that maps the subspace spanned by $\{|a_j^x\rangle\}$ onto itself. The operator σ^x and the corresponding subspace have a dynamic definition. That definition covers a certain period, which represents a sliding progression window.

The second order partial differential equation for a single embedding event is:

$$\nabla_0\nabla_0\psi \pm \langle\boldsymbol{\nabla},\boldsymbol{\nabla}\rangle\psi = \xi \tag{1}$$

The $\pm$ sign switches between quaternionic and Maxwell based differential calculus. This second order partial differential equation is integrated over the full generation cycle. As a consequence the equation for an averaged version χ of continuum ψ is obtained.

$$\nabla_0\chi = \int_{t_n}^{t_{n+1}} \frac{\partial^2\psi}{\partial t^2}\,dt \tag{2}$$

$$\zeta = \int_{t_n}^{t_{n+1}} \xi\;dt \tag{3}$$

$$\nabla_0\chi \pm \langle\boldsymbol{\nabla},\boldsymbol{\nabla}\rangle\chi = \zeta \tag{4}$$

t represents τ or t. ζ represents the continuous location density distribution that represents the full swarm.

$$H\chi = \nabla_0\chi = \frac{\partial\chi}{\partial t} = \zeta \mp \langle\boldsymbol{\nabla},\boldsymbol{\nabla}\rangle\chi = \zeta \mp \frac{\partial^2\chi}{\partial x^2} \mp \frac{\partial^2\chi}{\partial y^2} \mp \frac{\partial^2\chi}{\partial z^2} \tag{5}$$

Here H is an equivalent of the Hamiltonian.

In the embedding continuum $\mathfrak{C}$, the traces of what happened are the emitted vibrations and shape keeping fronts that independent of the progression window keep proceeding. The spherical shape keeping fronts do not vanish, but they fade away. With them the deformation also fades away. However, the recurrent embedding process keeps this deformation alive in a dynamical fashion. It drags the deformation with the subspace that represents the corresponding module.

Only when they appear in huge numbers the faded spherical shape keeping fronts can form a noticeable influence. This may be the reason of the existence of dark matter.

The averaged Green's functions now indicate the averaged effects of the recurrent embedding on the deformation of ψ. The result is that the corresponding potential no longer represents a singularity.

In $\mathfrak{H}$ the dimension of the subspace that represents the set $\{a_j^x\}$ has a clear significance. In order to comprehend what this dimension and the spread of the set do to the function ψ we use the Green's function. The Green's function represents the influence of the embedding of a single point-like artifact into ψ. That artifact can be a landing point or a hop. For a single point-like artifact at location $\boldsymbol{x}'$ in otherwise isotropic conditions, the Green's function equals

$$g_j = 1/|\boldsymbol{x} - \boldsymbol{x}_j'|. \tag{6}$$

We integrate over the space that is covered by density distribution ξ. If ξ represents an isotropic Gaussian distribution, then N Green's functions contribute to the integral that will equal [7]:

$$\mathfrak{G}(\boldsymbol{x} - \boldsymbol{x_c}) = \sum_0^N \frac{1}{|\boldsymbol{x} - \boldsymbol{x}_j'|} \approx \int_V \frac{\xi(\boldsymbol{x}' - \boldsymbol{x_c})}{|\boldsymbol{x}' - \boldsymbol{x_c}|} d\boldsymbol{x}' = C\ N\ \frac{\mathrm{erf}(|\boldsymbol{x} - \boldsymbol{x_c}|)}{|\boldsymbol{x} - \boldsymbol{x_c}|} \tag{7}$$

$$\boldsymbol{x_c} = \frac{1}{N}\sum_0^N \boldsymbol{x}_j' \tag{6}$$

C is a normalization constant. Here N represents the number of elements in the $\{a_j^x\}$ set. Green's function g_j represents the effect of the embedding of the single element a_j^x.

$\mathfrak{G}(\boldsymbol{x} - \boldsymbol{x_c})$ represents the local contribution to the gravitation potential. The function on the right side is a smoothed version of this contribution. It represents the local impact on the embedding continuum $\mathfrak{C}$.

This indicates that subspace dimension N directly relates to mass, which together with the location density distribution ζ determines the strength of deformation of ψ, which locally describes embedding continuum $\mathfrak{C}$.

11.3.1 No singularity

The integration over a full cycle removes the singularities of the individual Green's functions. In the example, the resulting field is a smooth function.

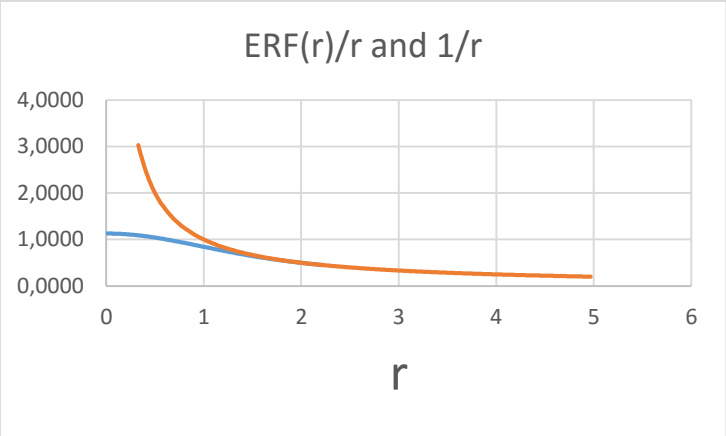

Figure 1. Close to the geometric center the singularities are converted in a smooth function. Further from the center the form of the Green's function is retained.

We suppose that this distribution is a good estimate for the structure of the swarm of a free electron. It is remarkable that this potential (the blue curve) has no singularity at $R = 0$. At the same time, already at a short distance of the center the function very closely approaches $1/R$ (the orange curve).

The term $\mathrm{ERF}(R)$ indicates the influence of the spread of the embedding locations. This view can be used to determine the spatially averaged effect of the single embeddings. The set $\{a_j^x\}_N$ corresponds to N instances of such spatially averaged contributions. This approach shows that deformation and thus mass is directly related to the size of the set and to dimension of the subspace that represents the module.

12 Attaching characteristics to a module

12.1 Module subspace

In free translation, the spectral theorem for normal operators that reside in a separable Hilbert space states: "If a normal operator maps a closed subspace onto itself, then the subspace is spanned by an orthonormal base consisting of eigenvectors of the operator." The corresponding eigenvalues characterize this closed subspace.

We take the closed subspace that is spanned by the eigenvectors of stochastic operator $\mathcal{O}^x$ as an example. These eigenvectors form a subspace of symmetry center $\mathfrak{S}_n^x$, which itself is a subspace. The mechanism $\mathfrak{M}_n$ takes care that a stochastic process attaches the proper eigenvalues to these vectors. The mechanism takes care that the set of eigenvalues $\{a_i^x\}$ obtains statistical characteristics that are typical for the elementary module type. The module gets its symmetry flavor, its electric charge, its color charge and its spin from the symmetry center. The map of the symmetry center to parameter space $\mathcal{R}^{⓪}$ gives the set $\{a_i^x\}$ its center location in $\mathcal{R}^{⓪}$ and indirectly in $\mathfrak{R}^{⓪}$. The embedding process gives swarm $\{b_i^x\}$, which is the image of $\{a_i^x\}$ in $\mathfrak{R}^{⓪}$ its mass.

The mechanism $\mathfrak{M}_n$ that controls the stochastic process, which fills the eigenspace of operator $\mathcal{O}^x$ with data determines the generation flavor of the elementary module.

12.1.1 Swarm characteristics

In this paper, we use the diversity that is represented by the standard model of contemporary physics as reference for naming elementary object types and their properties.

Elementary particle types have different masses. In the orthomodular base model this means that the corresponding closed subspaces have different dimensions and that correspondingly the swarms have different numbers of elements. It takes a type dependent number of progression steps for regenerating the corresponding swarm.

The swarm has a central location, which in separable Hilbert space is defined as the average $\boldsymbol{a}$ of the imaginary parts of the coherent set of source eigenvalues $\{a_i^x\}$. It is the geometric center of the local symmetry center. In the non-separable Hilbert space it is defined by the image $\wp(\boldsymbol{a})$, which is located in $\mathfrak{C}$. This target value corresponds to an object source location $\boldsymbol{a}$ in the flat parameter space of $\wp$. That parameter space is $\mathfrak{R}^{⓪}$.The source location may move as a function of progression.

The speed of transfer of information is set by the speed of information carriers. These information carriers are one-dimensional shape keeping fronts. The quaternionic second order partial differential equation describes the way in which these shape keeping fronts proceed.

In the continuum the observed image of the swarm cannot move faster than the speed with which information can be transported.

The statistical characteristics of the swarm and the symmetry related properties of the symmetry center are sources for the properties that characterize the types of the objects that are represented by the coherent swarm. The symmetry flavor, the symmetry related charge, the color charge and the spin of the object that is represented by the swarm are mainly set by the symmetry center on which the swarm resides.

Apart from the number of elements of the swarm, the properties of the swarm appear to depend on the generation flavor. The mechanism $\mathfrak{M}_n$ that generates the swarm determines this extra characteristic of the swarm.

12.1.1.1 Fermions

Fermions have half-integer spin. Fermions exist as elementary objects and as composites. All fermions have non-zero mass. This means that their embedding deforms the embedding continuum $\mathfrak{C}$.

Elementary fermions comprise electrons, quarks, neutrinos and their antiparticles. They are listed in the table in the chapter on symmetry flavor.

Embedding couples coherent swarms $\{a_i^x\}$ that possess the symmetry flavor of a symmetry center $\mathfrak{S}^x$ to an embedding continuum $\mathfrak{C}$ that has the symmetry flavor of reference operator $\mathfrak{R}^{⓪}$. If this symmetry flavor of the embedding continuum is fixed, then varying the symmetry flavor of the coherent swarm creates sixteen different elementary object types. Half of these types concern anti-particles. Again half of these sub-types concern left-handed quaternions and the other half are right-handed. Anisotropic types occur in three versions that are distinguished by the dimension in which the anisotropy occurs. Anisotropic types are marked by color charges. Isotropic types are colorless.

12.1.1.2 Massive Bosons

Bosons are known to feature integer spin. Massive bosons exist as elementary objects and as composites. Also massless bosons exist. Photons and gluons are massless bosons. The massless bosons do not deform the field in which they travel.

The difference of spin between massive elementary bosons and elementary fermions can be explained when the symmetry centers of fermions are generated in an azimuthal angle first and a polar angle second way, while the symmetry centers of bosons are generated in an polar angle first and an azimuthal angle second fashion. The polar angle takes 2π radians and the azimuthal angle takes π radians.

Fermions and massive bosons appear to contribute to a common gravitation potential. This means that bosons embed in the same embedding field as fermions do. Massive bosons couple to an embedding continuum in a similar way as fermions do. Boson swarms feature color-neutral symmetry flavors.

Massive bosons are observable as W_-, W_+ and Z particles. W_+ is the antiparticle of W_-. Until now, there is no indication of the existence of quark-like bosons. At least their "color" structure cannot be observed.

12.1.1.3 Spin axis

Fermion swarms and boson swarms contain a hopping path that can be walked into two directions. That hopping path may implement spin.

If the swarm is at rest (does not move), then the hopping path is closed. Relative to its symmetry center the swarm does not move, but it might oscillate.

For bosons the spin axis may be coupled to the polar axis. The polar angle runs from 0 through 2π. For fermions the spin axis may be coupled to the azimuth axis. The azimuthal angle runs from 0 through π.

Nothing is said yet about the fact and the corresponding influence that the number of hops can be even or odd. And nothing is said yet about whether the opening hop and the closing hop are coupled in a symmetric or asymmetric sense.

12.2 History, presence and future

In the orthomodular base model, the eigenvalues of the reference operators are not touched by management mechanisms or by the embedding process. Also historic eigenvalues are no longer touched by management mechanisms.

Presence is marked by a progression value that occurs in the real part of quaternionic eigenvalues of the category of well-ordered normal operators. History is marked by lower valued real parts of these quaternionic eigenvalues. ***Progression sensitive operators*** are members of the category of well-ordered normal operators and are characterized by the fact that they have known and fixed eigenvalues when the real part of the eigenvalue is lower than the present progression value. At the same time the current eigenvalues of these operators are influenced by the controlling mechanisms. ***Future*** eigenvalues of these operators are considered to be unknown. ***They belong to the non-observable part of the Hilbert space.*** The progression dependent management mechanisms have not yet touched these eigenvectors.

In the orthomodular base model ***presence, history and future are artificial concepts***. History is defined with respect to the current real value of the eigenvalues of the reference operators, which belong to the category of well-ordered normal operators.

The eigenspaces of ***progression sensitive operators*** exactly describe the history. ***The history is fixed***. Thus the historic eigenvalues are no longer touched by management mechanisms or by the

embedding process. However, these operators do not yet describe the ***future***. The future is constructed by the management mechanisms and the embedding process. This means that these mechanisms depend on the progression parameter***. The mechanisms only affect the current eigenvalues.*** These eigenvalues describe the presence.

Progression sensitive operators are related to functions that use a flat parameter space which is defined using the reference operators $\mathcal{R}^{⓪}$ and $\mathfrak{R}^{⓪}$ or indirectly by using the anti-Hermitian reference operator $\mathfrak{S}^{x}$ and a synchronization signal. The quaternionic screened Poisson equation uses such a synchronization signal.

The subspace that represents a module covers a sliding part of the last history. The dimension N of the subspace, which is covered by operator σ^{x} determines the number of covered progression instances. Inside the subspace progression rules the cyclic regeneration process. The subspace covers one cycle of that regeneration process. This period is governed by a controlling mechanism. N is smaller than the (fixed) dimension of the subspaces that represent the symmetry centers.

The progression window covers a recycling period in which the statistical properties of the set $\{a_j^x\}_N$ stabilize. This period is a property of the stochastic generation mechanism $\mathfrak{M}_n$. The stochastic generation mechanisms $\{\mathfrak{M}_n\}$ exist in a series of types that each have their own characteristics.

12.3 Model wide progression steps and cycles

Each closed subspace that represents a coherent swarm is governed by a mechanism $\mathfrak{M}_n$ that ensures dynamic and spatial coherence. In fact many different types of such mechanisms exist. They correspond to elementary particle types. If these modules combine into composites, then the generation cycles must synchronize. This asks for a model wide progression step that is much shorter than any swarm generation cycle. A Real Time Operating System-like scheduling mechanism must schedule the generation of composites from completed modules.

12.4 Swarm behavior

The coherent swarm moves as one unit. In fact, the represented object features three kinds of movement. The first kind stays internal to the swarm. During the corresponding generation process, the hopping speed has no significance for the movement of the swarm as a whole unit. The second kind is caused by the charge of the symmetry center in combination with the symmetry related field $\mathfrak{A}$. The third kind concerns the relocated swarm as a whole. This concerns the image $\{b_i^x\}$ of the original swarm $\{a_i^x\}$ onto reference space $\mathcal{R}^{⓪}$ or onto reference space $\mathfrak{R}^{⓪}$.The speed of this swarm makes physical sense.

Inside the swarm $\{b_i^x\}$, the represented object hops from swarm element to swarm element. The hopping path is folded and if the swarm is at rest, then the hopping path is closed. Adding extra hops to the original swarm $\{a_i^x\}$ causes movement of the $\{b_i^x\}$ swarm. Adding a closed string of hops in a cyclic fashion to swarm $\{a_i^x\}$ causes an oscillation of the $\{b_i^x\}$ swarm. From observations it follows that in composites, such as atoms only certain oscillation modes are tolerated. Adding an arbitrary open string of hops may open the hopping path in swarm $\{b_i^x\}$. In that case the sum of all hops is no longer zero. As a consequence the swarm $\{b_i^x\}$ will move. This motion gets its origin in the separable Hilbert space. The motion is mapped onto the continuum. The total movement is recognizable relative to the parameter space $\mathfrak{R}^{⓪}$.

A dynamic local change of the mapping function $\wp$ may move the swarm relative to other swarms. Such changes may occur when discrete objects deform the embedding continuum. Or if the symmetry related field $\mathfrak{A}$ relocates the local symmetry center. The third kind of movement gets its

origin in the non-separable Hilbert space. Relative to the parameter space, only the effect of the relocation is recognizable.

12.4.1 Partial creation and annihilation

Removing a string of hops from the hopping path can be interpreted as a partial annihilation occurrence. Thus, part of the object is temporary converted into an information messenger, which travels with optimal speed away from its source. Complete annihilation does not occur this way. Complete annihilation involves annihilation of the symmetry center.

Adding a string of hops to the hopping path can be interpreted as a partial generation occurrence. Thus, an information messenger is temporary converted into a new part of the object. Complete creation does not occur this way. Complete creation involves creation of the symmetry center.

12.5 Mass and energy

12.5.1 Having mass

Having mass can be interpreted as the capability to deform the continuum that embeds the concerned object. More mass corresponds to more deformation.

The fact that fermions and massive bosons contribute to a common gravitation potential means that they deform the same embedding continuum.

The dimension of the closed subspace, which in the separable Hilbert space $\mathfrak{H}$ represents a discrete object has a physical significance. Any eigenvector that contributes to spanning the closed subspace increases the dimension of the subspace. If all elements of the swarm contribute separately to the deformation of the embedding continuum, then the total deformation is proportional to the dimension of the subspace. In that case, this dimension relates to the mass of the object that corresponds to the swarm. If extra hops are added that cause movements or oscillations, then this adds to the mass in the form of kinetic energy. The extra hops may enter or leave in strings. Inside the swarm the hops that cause oscillation are stored as closed strings. Outside of the swarm the strings of hops are open and appear as information messengers.

12.5.2 Information messengers

Information messengers represent open strings of hops. At the same time they are solutions of the homogeneous second order partial differential equation. This means that they can be viewed as strings of one dimensional shape keeping fronts. One dimensional shape keeping fronts do not diminish their amplitude as function of the distance to their emission point. In an otherwise flat continuum the one dimensional shape keeping fronts and thus the information messengers proceed with the speed of information transfer. The energy carried by information messengers is proportional to the number of one-dimensional shape keeping fronts that they contain. If the duration of emission, absorption and passage is fixed, then the apparent frequency of information messengers is proportional to their energy.

In contemporary physics the information messengers are known as ***photons***. Photons are known to be able to cross huge distances and then still have sufficient amplitude left in order to be detected by suitable detectors. Messengers do not lose their amplitude. From experiments we know that the energy of photons is proportional to their frequency. Thus if photons are information messengers then this suggests that at least locally, the emission, the absorption and the passage of information messengers takes a fixed number of progression cycles.

Spurious one-dimensional shape keeping fronts may not be detectable via experiments. Large numbers of spurious one-dimensional shape keeping fronts may represent dark energy.

12.5.3 Red-shift

Red-shift is observed by photon detectors with photons that arrive from huge distances. This effect may be due to the fact that the second order partial differential equation does not hold for these huge ranges. If the period of emission is longer than the period of absorption, then some shape keeping fronts will be missed and may proceed as messengers that contain less shape keeping fronts or these messengers will be converted in kinetic energy of the absorbing object. The primary absorption will count a number of shape keeping fronts than originally were emitted. It means that the frequency is red-shifted.

Other interpretations make the Doppler effect responsible for the red-shift. The Doppler effect considers the absorbed objects as planar waves.

12.5.4 Mass energy equivalence

Creation and annihilation of elementary particles shows the equivalence of mass and energy.

12.5.4.1 Suggested creation process

Creation of elementary particles starts with the combination of two photons that came from opposite directions into an intermediate object. The intermediate object is a very short lived massive object that consists of as many paired elements as shape keeping fronts are contained in the constituting photons. The shape keeping fronts will convert into hops. The long chain of paired hops will then rip apart into two folded hopping strings that each form a coherent location swarm. Next the two swarms will split and move in opposite directions. At some instant in this procedure two symmetry centers are generated that will carry the generated particles.

12.5.4.2 Suggested annihilation process

Annihilation of elementary particles starts with the combination of an elementary particle and its anti-particle that come from opposite directions into an intermediate object. The intermediate object is a very short lived massive object that consists of as many paired elements as elements are contained in the constituting coherent location swarms. As part of the procedure the corresponding symmetry centers are annihilated. The hops will convert into shape keeping fronts. The long chain of paired shape keeping fronts will then rip apart into two separate chains of shape keeping fronts. Next these photons leave in opposite directions.

13 Relation to the wave function

The concept of wave function is used by contemporary physics in order to represent the state of a quantum physical object. The wave function is a complex amplitude probability distribution. Its squared modulus is a normalized density distribution of locations where the owner of the wave function can be detected. The value of this continuous distribution equals the probability of finding the owner at the location that is defined by the value of the parameter of the distribution.

If the detection is actually performed, then the object will be converted into something else. By the adherents of the Copenhagen interpretation, this fact is known as “the collapse of the wave function”.

The normalized density distribution of locations where the owner of the wave function can be detected corresponds to the map of a coherent swarm on a flat continuum eigenspace of the companion operator in the orthomodular base model.

Thus, the concept of the coherent map of a well-ordered coherent set on a flat continuum eigenspace of the companion operator in the orthonormal base model leads directly to an equivalent of the concept of the wave function in contemporary physics. Both concepts cannot be verified by

experiments. The equivalence indicates that the suggested coherent map extension of the orthomodular base model runs in a sensible direction.

The continuous density distribution does not play an active role in the model. It is only constructed for administrative purposes. Each of the swarm elements corresponds to an individual embedding occurrence. The continuous density distribution is used to compute the embedding potential. That potential can also be computed by using the squared modulus of the wave function in a similar way.

14 Traces of embedding

14.1 Embedding potential

The actual embedding of a discrete eigenvalue a_j^x in the embedding continuum does not last longer than a single progression step. For each object, the embedding occurs only once at every used progression step. The source eigenvalue a_j^x is taken by the controlling mechanism $\mathfrak{M}_n$ from the local symmetry center and is stored in the eigenspace of the location operator $\mathcal{o}^x$ that resides in the separable Hilbert space. Immediately afterwards the mechanism releases the embedding and replaces it by another embedding of a source eigenvalue, which it takes from a slightly different location a_{j+1}^x. This new source location is mapped onto its target location in the embedding continuum. This recurrent embedding process generates the map of the well-ordered coherent set of source eigenvalues $\{a_j^x\}$.

In the non-separable Hilbert space the map $\{\wp(a_j^x)\}$ affects the target subspace of the continuum eigenspace. This is done in a special way. Locally, the effect is determined by the ***non-homogeneous second order partial differential equations***. This holds both for the quaternionic version and for the Maxwell based version.

The homogeneous second order partial differential equation and the Poisson equation are restrictions of the non-homogeneous second order partial differential equation. The homogeneous second order partial differential equation controls the situation just before and just after the actual embedding action. The Poisson equation determines the situation during the actual embedding action. The embedding results in the emission of a 3D ***shape keeping front***. The solution of the Poisson equation ***deforms*** the target subspace of the embedding continuum. After release of the embedding, the 3D shape keeping front keeps proceeding, but it will quickly diminish its amplitude as function of the distance to the emission location.

The effects of the solutions of the non-homogeneous second order partial differential equations for all participating elements of the swarm combine and form an ***embedding potential***. The embedding potential represents a smoothed and averaged local view on continuum $\mathfrak{C}$.

In general can be said that the embedding of discrete artifacts trigger vibrations and deformations of the embedding continuum. The vibrations can be shape keeping fronts and oscillations and are solutions of the homogeneous second order partial differential equation. These solutions are restricted by local conditions and by the configuration of the triggers. For free particles these solutions are isotropic in one, two or three dimensions. In atoms the embedding of the electrons determine the configuration of triggers that cause spherical harmonics as solutions of the homogeneous wave equation. In that case the wave equation describes the behavior of the embedding field, rather than the behavior of the symmetry related field $\mathfrak{A}$.

14.2 Symmetry related potential

All elements of the coherent swarm are taken from the same symmetry center and have for that reason the same symmetry flavor. Embedded symmetry centers have their own dynamics, which is controlled by the symmetry related field $\mathfrak{A}$. Only the elements of the coherent swarm will be embedded in the embedding continuum. The effects of symmetry flavor coupling work over the whole reach of the symmetry center and thus over the whole reach of the coherent swarm. In the embedding continuum the source of this influence is located at the target value of the mapping function $\wp(\boldsymbol{a})$. The symmetry related charge at this location depends on the difference between the symmetry flavor of the coherent swarm and the symmetry flavor of the embedding continuum.

Also here the quaternionic second order partial differential equation describes what happens, but the charge stays at its center location. The governing equation is:

$$(\nabla_0\nabla_0 \pm \langle \boldsymbol{\nabla}, \boldsymbol{\nabla} \rangle)\, \varphi(q) = \sum_n \mathcal{g}(q, \mathrm{n}) \tag{1}$$

Here φ represents the quaternionic symmetry related potential and $\mathcal{g}$ represents the distribution of symmetry related charges and currents. In general $\mathcal{g}$ cannot be described by a continuous location density distribution.

For the static symmetry related potential this reduces to

$$\langle \boldsymbol{\nabla}, \boldsymbol{\nabla} \rangle \varphi(\boldsymbol{q}) = \sum_n \mathcal{g}(\boldsymbol{q}, \mathrm{n}) \tag{2}$$

Function $\mathfrak{C}(q)$ maps both φ and the eigenspace of $\mathcal{g}$ onto continuum $\mathfrak{C}$.

14.2.1 Difference with gravitation potential

The symmetry related potential deviates in many aspects from the gravitation potential. Where every element of the swarm contributes separately to the gravitation potential, will the local symmetry related potential only depend on the symmetry flavor of the complete swarm. It is generated by the symmetry center and not by the separate elements of that center. The virtual location of the electrostatic charge coincides with the location of the center of symmetry of the swarm. For elementary particles, the strength of the symmetry related potential does not depend on the number of involved swarm elements. The charge is set by the symmetry center on which the elementary particle resides.

The gravitation potential only implements attraction between the massive objects. The symmetry related potential implements repel between equally signed charges and implements attraction between differently signed charges.

14.3 Inertia

14.3.1 Field corresponding to symmetry center

Dedicated mechanisms use symmetry centers as resource for the generation of the locations of elementary particles. Symmetry centers are interesting as a subject for studying inertia. They have a spherical shape and a finite active radius. The activity of the mechanisms can be characterized by a normalized continuous density distribution. As an example we apply a Gaussian density distribution.

$$\rho(\boldsymbol{r}) = \frac{Q}{2\pi\, \sigma^3 \sqrt{2\pi}} \exp\left(-\frac{|\boldsymbol{r} - \boldsymbol{r}'|^2}{2\sigma^2}\right) \tag{1}$$

Here $\boldsymbol{r}'$ is the location of the center of the symmetry center. The produced distribution moves together with the symmetry center.

The potential of a Gaussian density distribution $\rho(r)$ equals:

$$\varphi_0(\boldsymbol{r}-\boldsymbol{r}') = \frac{Q}{4\pi r^2}\operatorname{erf}\left(\frac{r^2}{\sigma\sqrt{2}}\right)(\boldsymbol{r}-\boldsymbol{r}') \approx \frac{Q(\boldsymbol{r}-\boldsymbol{r}')}{4\pi r^2} \text{ for large } r = |\boldsymbol{r}-\boldsymbol{r}'|. \tag{2}$$

Here r stands for $|\boldsymbol{r}-\boldsymbol{r}'|$.

This is not the electric potential. This potential is generated in a background embedding field $\mathfrak{C}$ due to the recurrent temporary embedding of artifacts that are taken from the symmetry center. This can be shown by computing the double differential of $\varphi_0(\boldsymbol{r})$:

$$\frac{\partial \operatorname{erf}(ar)}{\partial r} = \frac{2a}{\sqrt{\pi}}\exp(-a^2r^2) = \frac{2}{\sigma\sqrt{2\pi}}\exp\left(-\frac{r^2}{2\sigma^2}\right);\ a = \frac{1}{\sigma\sqrt{2}} \tag{3}$$

$$\frac{1}{r^2}\frac{\partial}{\partial r}\left(r^2\frac{\partial\left(\frac{\operatorname{erf}(ar)}{r}\right)}{\partial r}\right) = \frac{2a^2}{\sqrt{\pi}}\exp(-a^2r^2) = \frac{1}{\sigma^2\sqrt{\pi}}\exp\left(-\frac{r^2}{2\sigma^2}\right) \tag{4}$$

The plot of the potential proves that this potential has no singularity. It is smooth near the center point.

The gradient of the potential equals:

$$\begin{aligned}\boldsymbol{\nabla}\varphi_0 &= \frac{\partial\varphi_0}{\partial r}\frac{\boldsymbol{r}-\boldsymbol{r}'}{r} \\ &= -\frac{Q}{4\pi r^2}\operatorname{erf}\left(\frac{r}{\sigma\sqrt{2}}\right)\frac{\boldsymbol{r}-\boldsymbol{r}'}{r} + \frac{Q}{2\pi r\sigma\sqrt{2\pi}}\exp\left(-\frac{r^2}{2\sigma^2}\right)\frac{\boldsymbol{r}-\boldsymbol{r}'}{r}\end{aligned} \tag{5}$$

The potential φ_0 adds on top of the average value of the embedding field $\mathfrak{C}$. If the observer position $\boldsymbol{r}$ moves with speed $\boldsymbol{v}$ relative to the embedding continuum $\mathfrak{C}$ then as a consequence a corresponding contribution to the vector potential:

$$\mathfrak{C}(\boldsymbol{r}) = \overline{\mathfrak{C}_0}(\boldsymbol{r})\,\boldsymbol{v}$$

appears to exist. $\overline{\mathfrak{C}_0}(\boldsymbol{r})$ is the average scalar part of the embedding field $\mathfrak{C}(\boldsymbol{r})$. Thus, locally:

$$\mathfrak{C}_0(\boldsymbol{r}) = \overline{\mathfrak{C}_0}(\boldsymbol{r}) + \varphi_0(\boldsymbol{r}-\boldsymbol{r}')$$

$$\mathfrak{C}(\boldsymbol{r}) = \overline{\mathfrak{C}_0}(\boldsymbol{r})\,\dot{\boldsymbol{r}}$$

$$\boldsymbol{\nabla}\overline{\mathfrak{C}_0} \approx \mathbf{0}$$

At the observer point the embedding continuum equals:

$$\mathfrak{C} = \overline{\mathfrak{C}_0}(\boldsymbol{r}) + \varphi_0(\boldsymbol{r} - \boldsymbol{r}') + \overline{\mathfrak{C}_0}(\boldsymbol{r})\,\dot{\boldsymbol{r}} \tag{6}$$

The scalar and vector potentials go together with a field $\mathfrak{E}$:

$$\mathfrak{E}(\boldsymbol{r}) \equiv -\frac{\partial}{\partial\tau}\mathfrak{C} - \boldsymbol{\nabla}\mathfrak{C}(\boldsymbol{r}) = -\overline{\mathfrak{C}_0}(\boldsymbol{r})\,\ddot{\boldsymbol{r}} - \boldsymbol{\nabla}\,\varphi_0(\boldsymbol{r} - \boldsymbol{r}')$$

$$= -\overline{\mathfrak{C}_0}(\boldsymbol{r})\,\ddot{\boldsymbol{r}} + \frac{Q}{4\pi r^2}\,\mathrm{erf}\left(\frac{r}{\sigma\sqrt{2}}\right)\frac{\boldsymbol{r}}{r} - \frac{Q}{2\pi r\sigma\sqrt{2\pi}}\exp\left(-\frac{r^2}{2\sigma^2}\right)\frac{\boldsymbol{r}}{r}$$

For large $r = |\boldsymbol{r} - \boldsymbol{r}'|$

$$\mathfrak{E}(\boldsymbol{r} - \boldsymbol{r}') \approx -\overline{\mathfrak{C}_0}(\boldsymbol{r})\,\ddot{\boldsymbol{r}} + \frac{Q}{4\pi}\boldsymbol{\nabla}\left(\frac{1}{|\boldsymbol{r} - \boldsymbol{r}'|}\right) = -\overline{\mathfrak{C}_0}(\boldsymbol{r})\,\ddot{\boldsymbol{r}} + \frac{Q}{4\pi|\boldsymbol{r} - \boldsymbol{r}'|^3}(\boldsymbol{r} - \boldsymbol{r}') \tag{8}$$

Here again $\boldsymbol{r}'$ is the geometric center of the symmetry center. Both the acceleration $\ddot{\boldsymbol{r}}$ and the nearness of the artifact with strength Q determine the extra field $\mathfrak{E}$. The first term on the left represents what is usually is experienced as inertia. The second term represents what is usually is experienced as gravitation.

In his paper “On the Origin of Inertia”, Denis Sciama used the idea of Mach in order to construct the rather flat field that results from uniformly distributed charges [10]. He then uses the constructed field in order to generate the vector potential, which is experienced by the uniformly moving observer. Here we use the embedding field as the rather flat background field.

14.3.2 Forces between symmetry centers

Two different symmetry centers represent two different contributions to field $\mathfrak{E}$.

The forces between two symmetry centers are specified by.

$$\boldsymbol{F_{12}} = -\boldsymbol{F_{21}} = \frac{Q_1\,Q_2}{4\pi|\boldsymbol{r_1} - \boldsymbol{r_2}|^3}(\boldsymbol{r_1} - \boldsymbol{r_2}) \tag{9}$$

14.3.3 Rotational inertia

If the observer rotates with respect to the embedding field, then the observer experiences a curl that is defined by

$$\mathfrak{B} = \boldsymbol{\nabla} \times \boldsymbol{\varphi} \tag{1}$$

If the rotation changes, then this goes together with a rotation of the $\mathfrak{E}$ field, which counteracts the increase of the rotation.

$$\frac{\partial}{\partial \tau}\mathfrak{B} = -\boldsymbol{\nabla} \times \mathfrak{E} \tag{2}$$

In this case the observer experiences rotational inertia.

15 Overlapping and shared symmetry centers

Part of the binding of particles involves the overlapping of symmetry centers and it involves the sharing of overlapped symmetry centers by controlling mechanisms. The symmetry related charge, the color charge and the spin of the symmetry center play an important role. Also the fact that the produced location swarm must correspond to a continuous location density distribution and that this distribution must own a Fourier transform plays an important role. The continuity of the density distribution and the existence of the Fourier transform are considered by this paper as essential for keeping spatial and dynamic coherence. Together, these facts are the reason of existence of the Pauli principle.

Overlapping is restricted by a set of rules. When symmetry centers overlap, then they can be shared by the controlling mechanisms. Also this sharing must obey strict rules. For example the embedding continuum must be in conditions that are compatible with the pile of overlapping symmetry centers. One of the criteria is that it must reflect spherical harmonic oscillations in accordance with a subset of the accumulated symmetry centers. The symmetry related charges are not involved in these oscillations.

The fact that equally signed symmetry related charges repel, counteracts the overlay of such symmetry centers, but the fact that the overlay receives color neutrality appears to have a greater priority and is achieved by tri-state switching or by conjugation of the colored symmetry centers.

In general the overlap and sharing rules stimulate neutralizing of symmetry related charges and the rules stimulate color confinement. No pair of symmetry centers in the pile is allowed to represent particles that have the same symmetry flavor and the same half integer spin.

16 Field interaction

The symmetry related field $\mathfrak{A}$ interacts with the embedding field $\mathfrak{C}$. In the environment of an elementary particle this can be expressed by the Dirac equation.

$$\nabla\, \mathfrak{C} = \left(\mathfrak{C}(m + e\mathfrak{A})\right)^* = m\mathfrak{C}^* + e\mathfrak{A}^*\mathfrak{C}^* \qquad (1)$$

The real value e stands for the symmetry related charge of the local symmetry center. The symmetry center contributes an individual symmetry related field φ to the overall symmetry related field $\mathfrak{A}$.

The symmetry related field $\mathfrak{A}$ is deformed by the embedding field $\mathfrak{C}$.

17 Composites

Closed subspaces can combine into wider subspaces. If in the disjunction no eigenvectors of the location operator are shared between the constituents, then the constituents stay independent and keep their characteristics. Still superposition coefficients may rule the relative contribution of these properties. The properties are added per property type and these sums are not affected by the superposition.

17.1 Closed strings

Elementary particles are represented by coherent location swarms that also implement a folded hopping path. At rest this hopping path is closed. Adding extra hops may open the hopping path. This means that the sum of all hops may no longer equal zero. As a consequence the swarm moves. If a closed string of hops is added, then on average the swarm still stays at the same location, but at the same time the swarm oscillates. Such oscillations occur inside atoms.

The added hops act for the whole swarm as displacement generators. In this way, the corresponding quaternions can be supposed to act as superposition coefficients.

Other quaternionic superposition coefficients may act as rotators. Special rotators can switch the color charge of quarks. They do not affect color-neutral swarms.

17.2 Open strings

The closed strings of superposition coefficients enter and leave the composite as open strings.

Messengers are open strings that relate to particular swarm oscillations. They are known as ***photons***.

Messengers are also represented by strings of one-dimensional shape keeping fronts.

Gluons are open strings that relate to swarm rotations. They can switch the color charge of quarks

Color confinement stimulates that in composites the combined color charge is neutralized.

17.3 Binding

The potentials are a means to bind constituents of composites. Embedding potentials form pitches. If the particles move or oscillate, then the pitches become ditches.

The orthomodular base model suggests that at every progression step in every participating elementary particle only one swarm element is influenced by the currently existing potentials.

17.3.1 Gravitation

In the orthomodular base model, this is obvious for the gravitation potential which describes the deformation of the embedding continuum that is caused by these constituents. All embedding events contribute separately to the deformation of the embedding continuum. The constituents produce pitches into the embedding continuum and when they oscillate or rotate these pitches transform into ditches. The strength of the gravitation potential depends on the number and the coherence of the involved swarm elements.

17.3.2 Symmetry related potential

The origin of the symmetry related potential can also take a role in the binding of constituents, but this is questionable. The source of the symmetry related potential is probably located at the center of mass of the composite and is not located at the centers of mass of the constituents. If the sources of this potential would be located on the centers of mass of the constituents, then in case of oscillating constituents, this would result in ongoing emission of electromagnetic radiation.

17.4 Binding in Fourier space

In this paper binding between elementary modules is not yet touched in detail.

If binding between modules is considered, then it is sensible to pass to Fourier space and take the Fourier transforms of the quaternionic functions that represent the location density distributions. In this way the location probability density distributions become characteristic functions and convolutions that represent mutual blurring convert in “simple” multiplications. This is the approach that is applied in quantum field dynamics. It is also the approach that is applied in Fourier optics.

For example the second order partial differential equation for the embedding continuum and the corresponding continuity equations can be transformed to Fourier space.

$$\nabla^*\nabla\psi = \nabla_0\nabla_0\psi + \langle\boldsymbol{\nabla},\boldsymbol{\nabla}\rangle\psi = \rho \tag{1}$$

$$\phi = \nabla\psi \tag{2}$$

$$\nabla^*\phi = \rho \tag{3}$$

$$p^*p\,\tilde{\psi} = p_0p_0\,\tilde{\psi} + \langle\boldsymbol{p},\boldsymbol{p}\rangle\,\tilde{\psi} = \tilde{\rho} \tag{4}$$

$$\tilde{\phi} = p\,\tilde{\psi} \tag{5}$$

$$p^*\tilde{\phi} = \tilde{\rho} \tag{6}$$

17.4.1 Comparing to Fourier optics

In Fourier optics the lenses play the role of boundary conditions and the Fourier transform of the Point Spread Function is used as imaging quality characteristic for the lens. It is known as the Optical Transfer Function (OTF) of the lens. Thus the Point Spread Function acts as a kind of Green’s function for the lens. The Fourier transform of the target picture equals the product of the OTF and the Fourier transform of the object distribution. The OTF depends on the angular and chromatic distribution of the participating objects. The OTF also depend on the homogeneity of the phases of the participating probability waves. The OTF of a series of subsequent imaging components equals the product of the OTF’s of the separate components. This simple rule only holds for ideal conditions in which angular distributions, chromatic distributions and phase homogeneity play a negligible role.

Not only the modulus of the characteristic is important, but also the transfer of phases matters. The modulus determines what part of the energy of the investigated object is present in the direct vicinity of the center of the image. The phase transfer determines the dispersion of the wave package that constitutes the object. It depends on the location where the image is observed. Due to the fact that the swarm is recurrently regenerated, the dispersion does not play a significant role.

In quantum physics the generated swarm acts as a first imaging element It includes the starting conditions. The embedding continuum ψ presents the boundary conditions. Its Fourier transform $\tilde{\psi}$ acts as a corresponding mapping quality characteristic. In this way it forms the next component of the imaging chain. In rather flat conditions the Fourier transform of the Green's function of the embedding field acts as the imaging quality characteristic of this field. Together the Fourier transform of the location density distribution of the swarm and the (local) Fourier transform of the embedding continuum form the imaging quality characteristic of the moving particle(s). This quality characteristic qualifies the capability to keep the coherence of the particles and the composites.

17.5 Contemporary physics

Here we compare with results of contemporary physics.

17.5.1 Atoms

For stable composites, such as atoms, an ongoing emission of electromagnetic radiation is obviously not the case. Still the behavior of atoms with respect to absorption and emission of photons indicate that the electrons cause an oscillation in concordance with the patterns of spherical harmonics. However, this oscillation occurs in the embedding continuum and does not concern the "location" of the electron charges.

For atoms and its composites, the strength of the symmetry related potential does not depend on the number of involved swarm elements. That number influences the deformation of the field, which embeds the elementary particles that together constitute the atom.

The behavior of the shell of atoms is described by spherical harmonics that are solutions of the homogeneous second order partial differential equation. This equation describes vibrations of the embedding continuum. These vibrations are caused by (non-isotropic) recurrent embedding of the electrons. These vibrations are described by the Helmholtz equation that describes the local behavior of the embedding field.

17.5.2 Hadrons

In hadrons the situation is different. There the binding is also regulated by gluons. Gluons are capable of rotating quarks such that their color charge switches to another value. Gluons can join in strings. As rotators they act in pairs. Gluons do not affect isotropic swarms.

17.5.3 Standard model

In the standard model of contemporary physics the symmetry related potential that governs the binding of electrons in atoms is considered to be the electromagnetic potential.

The standard model suggests the existence of other potentials that implement weak and strong forces. Gluons play a role in the strong force. Massive bosons play a role in the weak force. Introducing strong and weak forces suggests that the potentials act on the full swarm and not on the individual swarm elements.

18 Tri-state spaces

Quaternions not only fit in the representation of dynamic geometric data. They also match in representing three-fold states such as the RGB colors of quarks and the three generation flavors of fermions. In all these roles the real part of the quaternion plays the role of progression. Thus quaternions can also be used to model neutrino flavor mixing.

Say that a property is distributed over three mutually independent modes and these modes exist in a combination that superposes these three modes.

The property distribution is characterized by p_x, p_y, p_z

$$\cos^2(\theta_x) = \frac{p_x}{p_x + p_y + p_z}$$

$$\cos^2(\theta_x) + \cos^2(\theta_y) + \cos^2(\theta_z) = 1$$

The angles $\theta_x, \theta_y, \theta_z$ indicate a direction vector $\mathbf{n} = \{n_x, n_y, n_z\}$ in three dimensional state space.

$$|n_x|^2 = \frac{p_x}{p_x + p_y + p_z}$$

$$\cos(\theta_x) = n_x;\ |\boldsymbol{n}| = 1$$

If state mixing is a dynamic process, then the axis along direction vector $\boldsymbol{n}$ acts as the rotation axis. The concerned subsystem rotates smoothly as a function of progression. This is not a rotation in configuration space. Instead it is a rotation in tri-state space.

The fact that quaternions can rotate the imaginary part of other quaternions or of complete quaternionic functions also holds for tri-states. The quaternions that have equal real and imaginary size play a special role. They can shift an anisotropic property to another dimension. They can play a role in tri-state flavor switching.

E.M. Lipmanov has indicated that generation flavor mixing is related to a special direction vector in ordered three dimensional space [16][17]. This singles out a direction vector in the 3D phase space. That direction vector is defined by the angles of this vector with respect to the base vectors of the Cartesian coordinate system of that phase space.

$$\cos^2(2\,\theta_{12}) + \cos^2(2\,\theta_{23}) + \cos^2(2\,\theta_{31}) = 1$$

$$\cos^2(2\,\theta_e) + \cos^2(2\,\theta_\mu) + \cos^2(2\,\theta_\tau) = 1$$

$$\cos^2(2\,\theta_u) + \cos^2(2\,\theta_c) + \cos^2(2\,\theta_t) = 1$$

$$\cos^2(2\,\theta_d) + \cos^2(2\,\theta_s) + \cos^2(2\,\theta_b) = 1$$

The projection of the direction vector on the coordinate base vectors appears to relate to generation masses. Generation flavor mixing is well known as a phenomenon that occurs for neutrinos when they travel through space.

In the orthomodular base model the rest mass of the elementary particle is related to the number of the elements in the location swarm that the mechanism $\mathfrak{M}_n$ picks from the symmetry center.

19 Conclusion

It appears sensible to suggest that physical reality mimics a network of mathematical structures that is used and controlled by a set of coherence ensuring management mechanisms. This setup aims at reducing relational complexity and it prevents dynamical chaos. The network consists of chains of structures that each start with a rather simple foundation. The major chain starts with an orthomodular lattice.

In this way an orthomodular base model emerges with inescapable evidence. This model treats all discrete objects as modules or modular systems that are embedded in continuums. This is supported by an infinite dimensional separable Hilbert space and a companion non-separable Hilbert space. Both Hilbert spaces act as structured storage media. The management mechanisms ensure the dynamic and spatial coherence. This leads to a model in which progression steps in the discrete part and flows in the continuous part of the model.

The introduction of symmetry centers enables the distinction between two fields that influence the kinematics of the discrete objects that appear as modules in the model. The symmetry centers house the artifacts that indirectly interact with the symmetry related field $\mathfrak{A}$.

The embedding process creates the triggers that deforms the embedding continuum in a dynamical way and causes vibrations in that continuum. Without these triggers the embedding continuum is not affected.

The symmetry related field $\mathfrak{A}$ can be considered to overlay the parameter space $\mathfrak{R}^{⓪}$ of the embedding continuum $\mathfrak{C}$ and features electric charges that are concentrated on the geometric centers of local symmetry centers. In spherical symmetric conditions this coincides with the local center of gravitation symmetry.

The habits and diversity of quaternions play an essential role in the extension of the orthomodular base model. These habits cause a variety of module types that differ in their properties and in their behavior. The generation of the modules is controlled by stochastic management mechanisms. The behavior of the modules and of the continuums is both initiated and restricted by the embedding process.

According to the model, history is precisely determined and stored in the Hilbert spaces. The controlling mechanisms act in a short period around the current progression value. Each mechanism acts in a sliding window that is represented by a closed subspace of the separable Hilbert space. The future is unknown, but it is restricted by the capabilities of the orthomodular base model and the by the controlling mechanisms.

This paper does not consider in depth the mutual binding of elementary modules. Nor does it treat the effects of arbitrary boundary conditions.

The development of mathematical tools that are used by physicists did not always occur in sync with the sometimes violent development of physical theories. Sometimes choices were made that would not have been taken when the proper mathematical tools were developed in an earlier phase. The paper shows that when looking back on this development , some leading physicists did not always provide the most sensible choice. They cannot be blamed for that choice, but as a consequence, the models of contemporary physics are more complicated than is necessary and do not reach as deep as is possible. It will be difficult to repair that situation.

If the target is to investigate the foundations of physical reality, then it is sensible to apply the most advanced mathematical tools and obey the restrictions that are set by these tools.

Appendix

20 Related historic discoveries and other references

Physical models use mathematical tools. The development of mathematical tools did not evolve in sync with the development of the physical models that use these tools. Complicated mathematical tools may take several decades before they mature.

[1] Quantum logic was introduced by Garret Birkhoff and John von Neumann in their 1936 paper. G. Birkhoff and J. von Neumann, *The Logic of Quantum Mechanics*, Annals of Mathematics, Vol. 37, pp. 823–843

[2] The lattices of quantum logic and classical logic are treated in detail in: http://vixra.org/abs/1411.0175 .

[3] The Hilbert space was discovered in the first decades of the 20-th century by David Hilbert and others. http://en.wikipedia.org/wiki/Hilbert_space.

[4] In the second half of the twentieth century Constantin Piron and Maria Pia Solèr proved that the number systems that a separable Hilbert space can use must be division rings. See: "Division algebras and quantum theory" by John Baez. http://arxiv.org/abs/1101.5690 and http://www.ams.org/journals/bull/1995-32-02/S0273-0979-1995-00593-8/

[5] Paul Dirac introduced the bra-ket notation, which popularized the usage of Hilbert spaces. Dirac also introduced its delta function, which is a generalized function. Spaces of generalized functions offered continuums before the Gelfand triple arrived.

[6] In the sixties Israel Gelfand and Georgyi Shilov introduced a way to model continuums via an extension of the separable Hilbert space into a so called Gelfand triple. The Gelfand triple often gets the name rigged Hilbert space. It is a non-separable Hilbert space. http://www.encyclopediaofmath.org/index.php?title=Rigged_Hilbert_space .

[7] Potential of a Gaussian charge density: http://en.wikipedia.org/wiki/Poisson%27s_equation#Potential_of_a_Gaussian_charge_density .

[8] Quaternionic function theory and quaternionic Hilbert spaces are treated in: http://vixra.org/abs/1411.0178 .

[9] In 1843 quaternions were discovered by Rowan Hamilton. http://en.wikipedia.org/wiki/History_of_quaternions

Later in the twentieth century quaternions fell in oblivion.

[10] http://en.wikipedia.org/wiki/Wave_equation#Derivation_of_the_wave_equation

[11] http://en.wikipedia.org/wiki/Yukawa_potential

[12] "The Dirac equation in quaternionic format"; http://vixra.org/abs/1505.0149

[13] "Quaternionic versus Maxwell based differential calculus"; http://vixra.org/abs/1506.0111

[14] The online EMFT book of Bo Thidé contains a formula section that treats vector calculus and vector differential calculus. http://www.plasma.uu.se/CED/Book/EMFT_Book.pdf .

[15] Different number systems and their arithmetic capabilities are treated in http://www.scorevoting.net/WarrenSmithPages/homepage/nce2.pdf.

[16] "Neutrino Oscillations"; http://www2.warwick.ac.uk/fac/sci/physics/current/teach/module_home/px435/lec_oscillations.pdf .

[17] "On Radical Ph-Solution of Number 3 Puzzle and Universal Pattern of SM Large Hierarchies"; http://arxiv.org/abs/1212.1417